View metadata, citation and similar papers at core.ac.uk
brought to you by CORE
provided by ScholarBank@NUS

SYSTEMATIC INVESTIGATION ON THE ULTRATRACE ANALYTICAL MONITORING OF ANIONIC SURFACTANTS ON SILICON WAFER SURFACE BY CAPILLARY ELECTROPHORESIS USING DESIGNED EXPERIMENTS

HOO SIEOW CHENG *(BSc, NUS)*

A THESIS SUBMITTED

FOR THE DEGREE OF MASTER OF SCIENCE

DEPARTMENT OF CHEMISTRY

NATIONAL UNIVERSITY OF SINGAPORE

2004/05

Acknowledgements

Foremost, I would like to express my most sincere gratitude to my supervisor, Professor Li Fong Yau, Sam for his invaluable advice and patience throughout this research.

I am thankful to Dr. Thomas Ehmann for initiating this project and guidance throughout the project development.

I am grateful to Siltronic Singapore Pte Ltd. for providing me the financial support to carry out this research.

Finally, I wish to especially thank my beloved family for their constant support and help one way or another, without them this project would not be possible.

Summary

Surfactants are used intensively in the semiconductor wafer manufacturer. It promotes cleanliness and maintains the purity of the surface of silicon wafers, which is an important parameter to monitor regularly for high yield of semiconductor devices in a production line. Surfactants as dodecylbenzene sulfonate (DBS) are commonly added as main additives as cleaning agents. There are many publications on the determination of anionic surfactant by capillary electrophoresis (CE). An appropriate system with sub-ppb detection that tolerates a hydrofluoric acid matrix is not yet established. In the first part of this report, a robust method for the analysis of DBS is established by designed experiments by Taguchi methodology. This systematic optimization tool greatly facilitates method development by minimizing the number of experiment yet produces a randomized test matrix in determining the main factors. A noise parameter as hydrofluoric acid (HF) is incorporated to develop a more robust system. Eighteen experiment (L_{18}) and a confirmation run determine a set of parameters and levels for the analysis of DBS. The experiments are evaluated by calculating the S/N values with four responses. The second part of this report includes the optimization of DBS analysis to ultra trace level. This optimized system is essential for monitoring of surfactant residue in the wafer surface, which may cause detrimental effects on the electronic devices. Again, Taguchi methodology is used to design a sixteen-test experiment (L_{16}) to determine the main parameters to improve the detection limit. Together with the high-resolution detector cell and the optimized system, the LOD and LOQ of DBS analysis are 6 ppb and 26 ppb respectively. The QC and spike percent recovery of DBS is 80 to 108% with 95% confidence limit.

List of Publication

Systematic Parameter Screening for Capillary Electrophoresis Monitoring of Surfactants on Silicon Wafer Surfaces by Designed Experiments.

Submitted to Journal of Chromatographic Science.

List of Figures

List of Tables

Content

1. Introduction

1.1 Surfactant

Surface preparation is one of the many key processes in a wafer manufacturing plant. Good quality wafers undergo series of cleaning processes to maintain the surface purity by removing contaminants such as metallic and particles. Surfactants are used to enhance the wettability of wafer surface, improving the removal efficiency of particles. A definition of surfactant is "a substance that lowers the surface or interfacial tension of the medium in which it is dissolved" [1]. Surfactants are made up of hydrophobic groups and hydrophilic groups, and divided into four categories according to the ionization of the hydrophilic groups. Surfactants containing positive ions such as $R\text{-}SO_3^-$ are called anionic surfactants; those containing negative ions such as $R\text{-}NH_3^+$ are called cationic surfactants; those hydrophilic groups which are not ionised are called non-ionic surfactants; and those are containing both positive and negative ions are amphoteric surfactants [2]. In final wafer cleaning process, acidic solution, especially due to the hydrofluoric acid (HF) results Si wafer surfaces with a negative zeta potential, and the Si_3N_4 surface shows a positive potential. Therefore, if a charge particle exists in the cleaning solution, deposition on one of the surfaces will occur. Surfactants are added to these acidic cleaning solutions, to minimise the particles adhering to the wafer surfaces [3]. Traces of surfactant, as organic contaminants, retained on the wafer surface will cause detrimental effects such as increased leak current, hampering gate oxide performance on electronic device [3]. Consequently, a routine method for monitoring surfactants is necessary. Dodecylbenzene sulfonate (DBS) was chosen as a model surfactant as anionic alkyl

benzene sulfonates are widely used in surfactant formulation because of its bio-degradability [4]. There are many researches on analytical methodology [2] and published literatures on the analysis of surfactants, particularly emphasis on alkylbenzene sulfonate [4]-[16]. Separation techniques like atomic absorption spectrophotometry (AAS) [4], electrophoresis using aqueous gel [5], high-resolution gas chromatography/mass spectrometry (GC/MS) [6], gas-liquid chromatography / mass spectrometry (GLC/MS) [7], high performance liquid chromatography (HPLC) [8] [9] and capillary electrophoresis (CE) [10]-[16].

CE is becoming more widely used as a micro/trace analytical technique especially for anions. As compared to other chromatographic techniques, CE offers more advantages for this purpose, e.g. low consumption of chemicals and analytes as well as high resolution. Moreover, CE is easy to operate, fast and robust. Th. Ehmann *et al*. has successfully established a routine analysis method for anions and cations on silicon surface using CE technique [16]-[19]. In the semiconductor industry where high purity of silicon wafer surface is of greater demand, a routine and robust analysis for anionic surfactant on silicon surface is becoming crucial.

1.2 High performance capillary electrophoresis (HPCE)

High performance capillary electrophoresis (HPCE) is a highly sensitive analytical technique that produces accurate and precise data for qualitative and quantitative analysis. The growing popularity for using HPCE in different disciplines such as chemical, biomedical, pharmaceutical and semiconductor industries due to its fast and

high efficiency applications [20]. In particular in semiconductor industry, the wafer sample solution is of minimum amount. HPCE is of advantage as the analysis requires small sample volume (~8 nL per injection) [18]. Separations of great molecular weight dynamic range including small ions, proteins, peptides, DNA are possible by HPCE. Applications in DNA sequencing, serum analysis, organic and inorganic ions, chiral separations have been demonstrated [20]-[24]. It is a separation technique based on the difference in ion linear velocity (v) in an electric field (E) as shown in (1).

$$v = \mu_E E \quad (1)$$

1.3 Basic Principle of HPCE

HPCE is a simple analytical machine where species of analytes are separated within a capillary under an electric field [22]. The basic components of a HPCE system are silica capillary, high voltage supply, constant temperature compartment, two electrolyte vials, a running buffer, and a detector (Figure 1.1). Sample is injected into the capillary via pressure or voltage at the anode end (Figure 1.2). After injection, the analytes interact with the wall of the capillary and/or the buffer, as the analytes move towards the detector either by the electroosmotic of flow (EOF) and the electrophoretic flow of the sample (E*ep*).

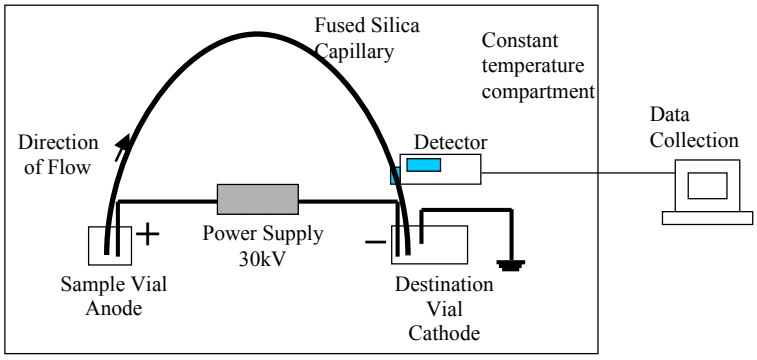

Figure 1.1: Schematic diagram of the basic components of a HPCE system.

A specific detector measures the positive or negative absorbance signal. Lastly, the identification and determination of the concentration of separated analytes will be analyzed by computer software. The software will typically calculate the peak area (Figure 1.3) based on half-width and migration time.

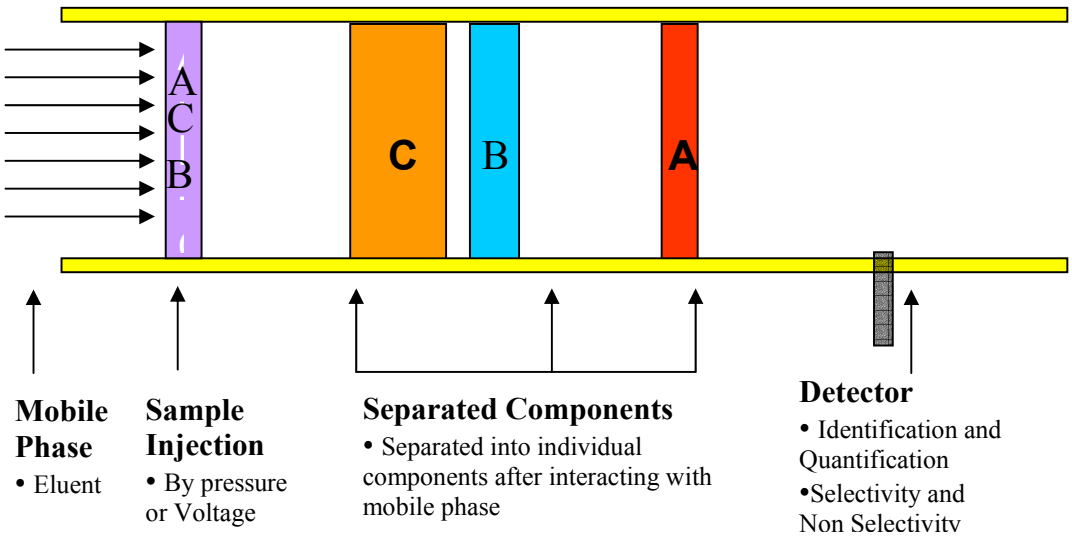

Figure 1.2: A schematic diagram of the separation of three analytes in a capillary.

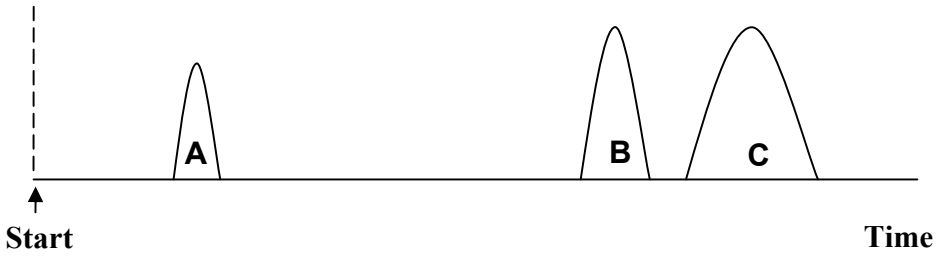

Figure 1.3: A diagram of a typical electrogram of HPCE analysis.

1.3.1 Mechanism of Separation

The silonal groups of a capillary are ionised by a high pH electrolyte replacing Si-OH to $Si\text{-}O^-$ at the inner surface of the capillary (Figure 1.4). The positive cations will be

attracted to the capillary forming the first layer called the *Fixed Layer*, and the mobile layer is the *Diffuse Double Layer* (Figure 1.5).

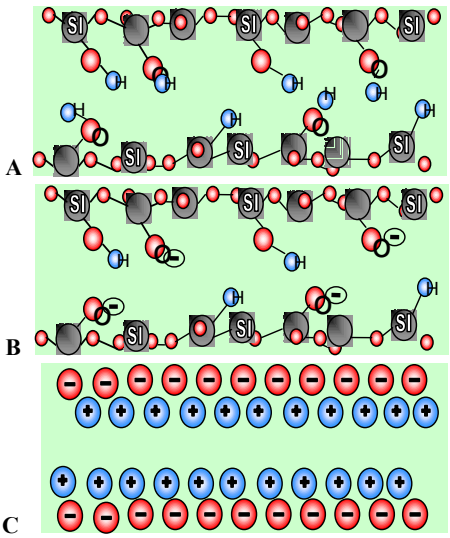

Figure 1.4A: Schematic diagram of capillary surface.

Figure 1.4B: Flushing of high pH running buffer, dissociation of silonal groups.

Figure 1.4C: Cations compensate from running buffer.

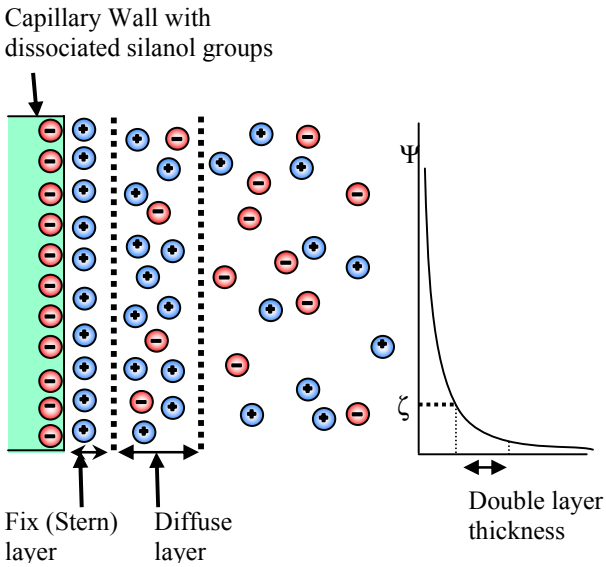

Figure 1.5: Schematic diagram of fix layer, diffuse layer and its zeta potential.

An electric field is applied across the capillary. The mobile layer is pushed toward the negatively charged cathode, resulting in an electroosmotic flow or EOF, i.e. "electrically-driven pump". The potential drops drastically until it reaches the zeta potential (ζ) at the diffused double layer zone, and declines gradually. EOF is proportional to zeta potential (charge on capillary surface) and this zeta potential is proportional to the thickness of the double layer (2):

$$\zeta = \frac{4\pi\delta e}{\varepsilon} \qquad (2)$$

where,

ζ = zeta potential
δ = thickness of diffuse double layer
e = charge per unit surface area
ε = dielectric constant

The movement of the electrolyte is called electroosmotic mobility, μ_{EOF}. Anions in the sample solution move against the EOF towards the anode, while cations move along with EOF towards the cathode. This movement of ions is called electrophoretic mobility, $\mu_{Ep.}$ Therefore mixtures of ions are separated based on the differences in electrophoretic mobilities. The cations moving along with EOF with combined μ_{EOF} and μ_{Ep} will migrate to detector faster than anions. Figure 1.6 illustrates the migration of a mixture of ions with the following sequence: cations, neutral and anions.

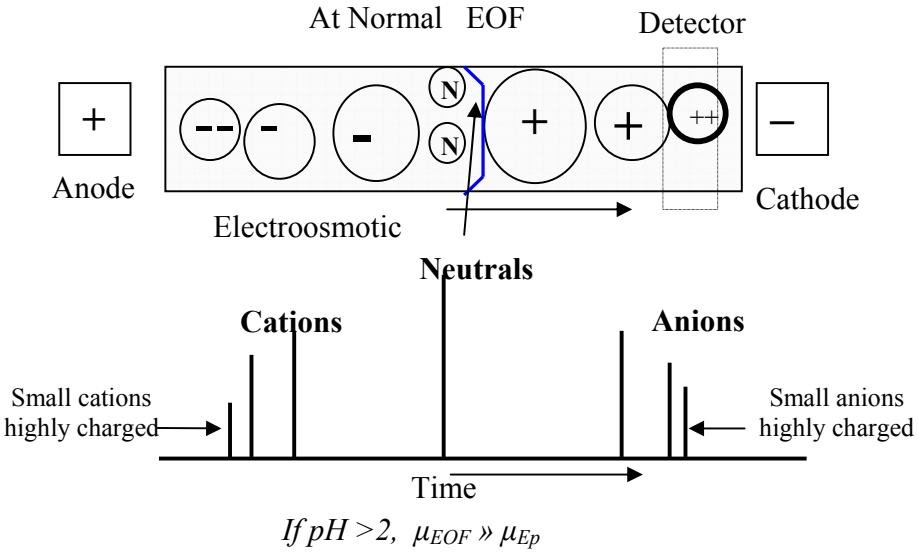

Figure 1.6: Illustration of separation of a mixture of ions by CE.

(The black lines show the different ions and the heights represent the concentration of the ions. Cations have the shortest migration time followed by neutral ions, and anions have the longest migration time.)

1.3.1.1 Separation by charge and viscosity

The basic mechanism for separation in HPCE is the difference in μ_{Ep}. The mobility is related to the dielectric constant, ε, and the viscosity of the ion (3) (4) [20]-[24].

$$\mu_{EOF} = \frac{\zeta\varepsilon}{4\pi\eta} \qquad (3)$$

where,

η = viscosity of buffer

from (2) and (3),

we obtained:

$$\mu_{EOF} = \frac{\delta e}{\eta} \qquad (4)$$

1.3.1.2 Separation by charge-to-mass

The separation of ions in CE is also based on the charge-to-mass ratio. The electric force, $F_{E,}$ is related to the product of ion charge, q, and the applied electric field, E (5). The frictional force, $F_{F,}$ present within the capillary depends on the size, viscosity and the radius of the ion (6). Since the amount of F_E applied is equal to the amount F_F required to counteract it, the mobility is directly related to the charge and inversely proportional to the viscosity and size of the ion (7) [24].

$$F_E = q\,E \qquad (5)$$

where,

F_E = Electric Force
q = Ion Charge
E = Applied Electric Field

$$F_F = -\,6\pi\eta r\,v \qquad (6)$$

where,

F_F = Frictional Force
r = ion radius

Rearranged (6),

$$q\,E = 6\pi\eta r\,v$$

$$\mu_E = \frac{q}{6\pi\eta r} \qquad (7)$$

1.3.2.4 Separation by velocity of electrolyte

For a non-charge neutral analyte, the migration is dependent on the velocity of the electroosmotic flow, v_{EOF}. v_{EOF} is caused by the applied electric field is indirectly proportional to the viscosity of the electrolyte (8) [24]. For an aqueous electrolyte, η is close to that of water; a neural analyte is eluted based on E, which is the voltage divided by the length of the capillary.

Rearrange (1) and (2),

$$v_{EOF} = \frac{\zeta\varepsilon}{4\pi\eta} E$$

$$v_{EOF} = \frac{\mu_{EOF} V}{L} \quad (8)$$

where,

V = applied Voltage
L = capillary length

The migration of a charged particle in an electrical field is determined by its charge-to-mass ratio, whereas the migration of a non-charged analyte is determined by the velocity of the electroosmotic flow, v_{EOF}, which is in turn dependent of the voltage and the length of the capillary [20].

1.3.2 Basic components of HPCE

The capillary is made up of silica. A layer of polyimide is coated on the outer surface of the capillary to improve its mechanical strength, i.e. to prevent the brittle, thin capillary from breaking. A typical capillary has dimensions of 50 and 375 μm inner and outer diameters (ID, OD) respectively (Figure 1.7).

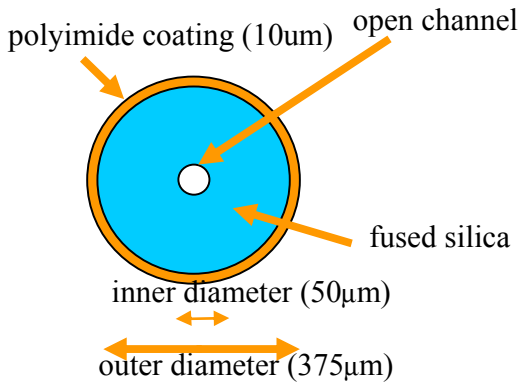

Figure 1.7: A schematic cross section diagram of a capillary.

The fluctuation in temperature will affect the viscosity of the sample, which will cause differences in sample injection and migration time. It is important to keep a constant temperature in capillary, so that reproducible results can be obtained. The capillary in HPCE usually comes with a closed fan system where the set temperature can be maintained to within ±0.1 degree Celsius to maintain a constant temperature and to dissipate Joule heat.

Similar to other spectroscopy technique, there are many choices of detectors to measure analytes based on their characteristic and sensitivity. Table 1.1 shows the list of detection method and an example of a detector [23]. Selective detector, e.g. UV detection, conductivity detector, are by far the most commonly used detectors [25]-[28]. Indirect UV detection[25][26][28] is employed for analytes that do not contain chromophores (i.e. non-UV active). Ionic chromophore materials, e.g. pyromellitic acid (PMA), are added into an aqueous running buffer. The presence of a non-UV active analytes, e.g. Na^+, replaces an ionic chromophore, thus reduction in UV absorbance (Figure 1.8).

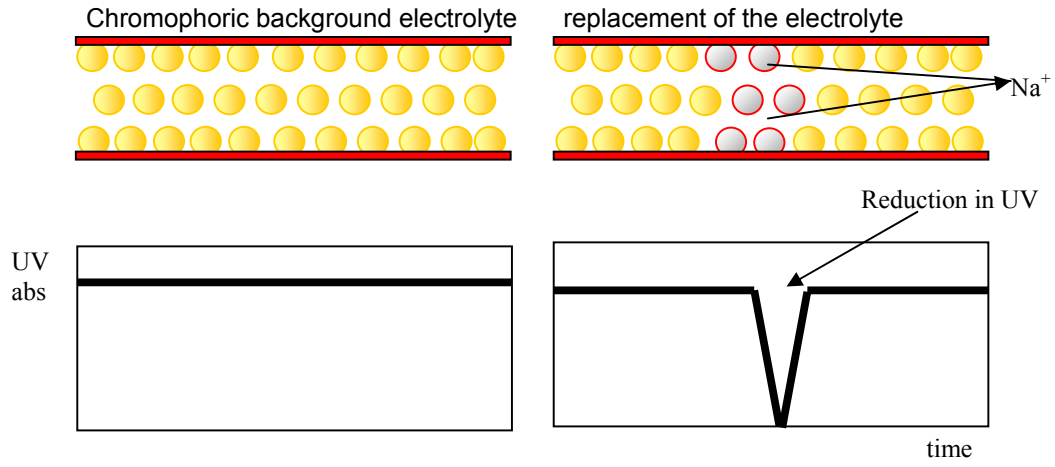

Figure 1.8: Schematic diagram of the mechanism of an Indirect UV detector.

Detection Method	**Example of detector**
Absorbance	UV/VIS, Diode Array Detection (DAD)
Electrochemical	conductivity, amperometry
Fluorescence	Laser Induced fluorescence Detection (LIF)
Mass spectrometric	Mass spectrometer

Table 1.1: Detection Methods and detectors of HPCE.

1.4 Modes of HPCE Operations

HPCE is a versatile analytical tool since it can analyse different types of samples in various industries. Optimization of separation is easy and analytes result in five basic modes of operation (Table 1.2 and Figure 1.9). A relevant application by these operations is summarised in Table 1.3.

Modes of Operation	**Basis of Separation**
CZE	Free solution
CGE	Size and Charge
CIEF	Isoelectric point
CITP	Moving boundaries
MECK/MECC	Hydrophobic/ionic interactions with micelles

Table 1.2: Summary of modes of Operation and their Basis of separation [24]

Small Ions	Small molecules	Peptides	Proteins	Oligo-nucleotides	DNA
CZE	MECC	CZE	CZE	CGE	CGE
CITP	CZE	CITP	CGE	MECC	
	CITP	MECC	CIEF		
		CIEF	CITP		
		CGE			

Table 1.3: Application of CE based in different modes of operations. [24]

1.4.1 Capillary zone electrophoresis (CZE)

CZE is the basic mode of HPCE. In the simplest form, the capillary is filled only with buffer. As the name implies, the separation of the ions is based on the migration in discrete zones due to the difference in mobilities and velocities (Figure 1.9A). Although it is a simple technique, many parameters can be changed to increase the selectivity and sensitivity [33],[36],[49],[50]. These parameters include buffer selection and concentration, pH, addition of modifiers like surfactants, solvents, cations etc, temperature and capillary wall modification.

1.4.2 Capillary gel electrophoresis (CGE)

The separation mechanism is adopted from the slab or tube gel electrophoresis [20],[23]. The greatest difference is that CGE is able to use10 to 100-times higher an electric field without the problematic Joules heating. CGE, like other HPCE modes, has an on-capillary detection system that greatly reduces the sample size and increase sensitivity. The advantage of automation stands out when compared with traditional slab gel electrophoresis. A typical CGE capillary contains a solid-like structure made up of a porous polymer, such as crosslinked polyacrylamide and agarose (Figure 1.9B).

1.4.3 Micellar electrokinetic capillary chromatography (MEKC or MECC)

MEKC is used widely in separating neutral species by the addition of surfactants in the running buffer [22],[31],[45]. Micelles are aggregated individual surfactant molecules, which are formed at or above the critical micelle concentration. The hydrophobic tails of the surfactant molecules orient towards themselves and the charged head towards the buffer (Figure 1.9E). The interaction between the micelle and the neutral solutes by partitioning in and out of the micelle leads to separation of the neutral analytes. The more hydrophobic species will stay with the micelle longer than in the buffer solution. For the charged ions, they migrate either with or against the EOF depending on the charge, hence, resulting in separation.

1.4.4 Capillary isoelectric focusing (CIEF)

CIEF is a high-resolution separation technique based on pI values. The capillary is made up of a pH gradient formed by using ampholytes. Ampholytes are molecules that have both an acidic and a basic end, called zwitterionic. They can have different pI values, at a range of pH solutions, (pH 3 – 9). The separation occurred when charged solutes and ampholytes migrate in the electric field until they become uncharged, which occurs at their pIs. This process is called ‘focusing’. The solute zone remain narrow since a solute which enters a zone of different pH will become charged and migrate back (Figure 1.9C). This method is widely used in protein separation [20][21].

1.4.5 Capillary isotachophoresis (CITP)

CITP is called the ‘moving boundary’ technique. The solute is sandwiched between two different solutions, a leading and a terminating electrolyte. The mixture is separated into zones (based on different mobilities within the mixtures) as they migrate at the same velocity as the two electrolytes (Figure 1.9D). This technique is special, as the solute is able to achieve steady-state velocity at different electric field by adjusting the mobility. This means that at the lowest electric field across the zone it has the highest mobility. With this, it is able to achieve very sharp zone between different solute [18] [53]. It is also interesting to that CITP is able to maintain constant concentration in each zone, determined by the concentration of the leading electrolyte. Zones that are less concentrated will be sharpened to adapt to the proper concentration. Since CITP is performed in a constant current mode, a constant ratio must exist between the concentration and the mobility of the ions in each zone. This is a popular pre-concentration step prior to CZE, MEKC, or CGE.

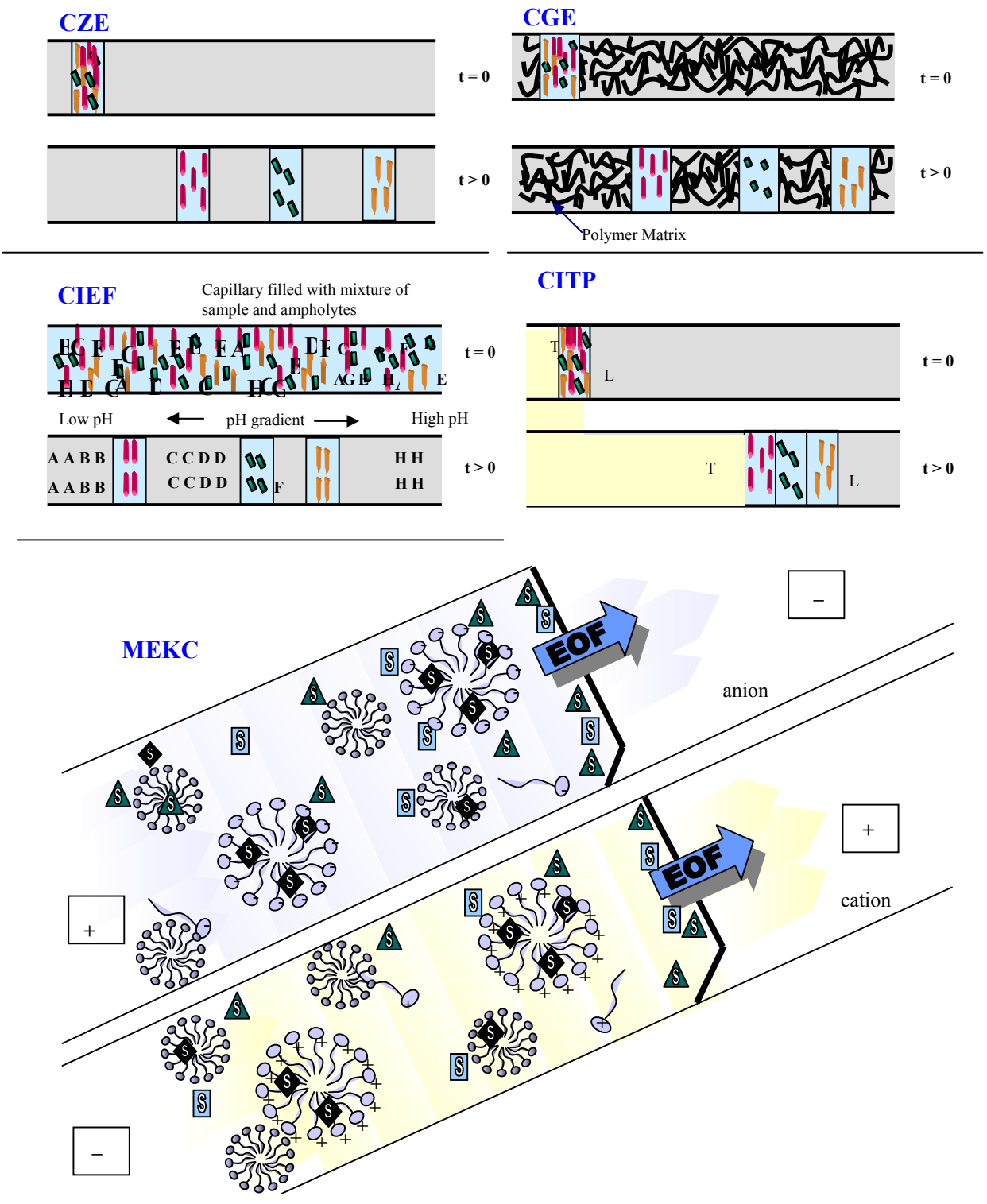

Figure 1.9: Different modes of CE applications.
A: CZE; B: CGE; C: CIFE; D: CITP; E: MEKC [24]

1.5 Factors Effecting EOF

1.5.1 Applied Voltage

Increase in voltage increases EOF, reduces migration times, and results in faster separation. Increasing voltage also increases separation efficiencies (Figure 1.10) provided heat (Joule heating) in the capillary is efficiently dissipated. The disproportionate increase of current with voltage (Figure 10) indicates a temperature increase [24].

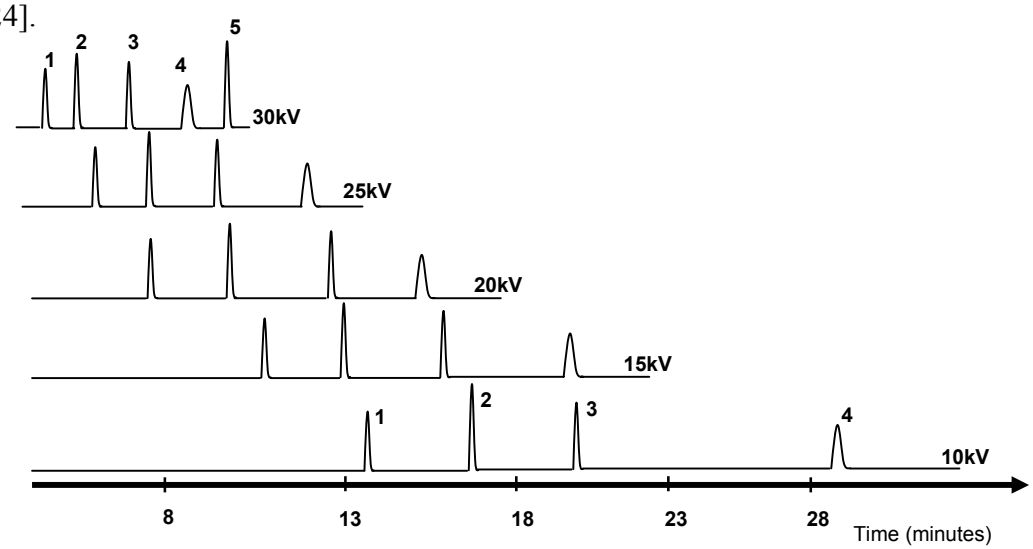

Figure 1.10: Electropherograms the effect of applied voltage on migration times.

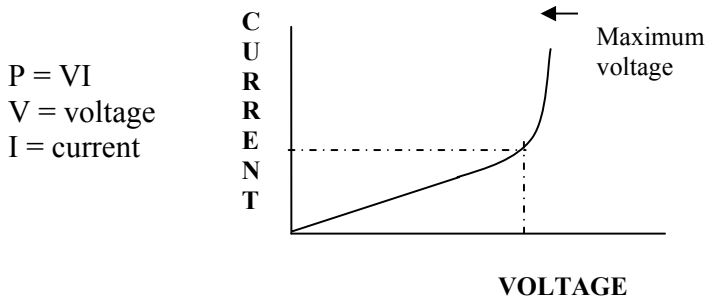

Figure 1.11: Maximum voltage by Ohm's Law.

1.5.2 Buffer pH

At High pH (6-8), there is more dissociation of Si-OH to $Si-O^-$, and greater zeta potential. EOF increases as the thickness δ increases. At lower pH (2-6), there is less surface ionization, therefore lower zeta potential, leading to lower EOF. At pH below pH 2, since there is no ionization of Si-OH to SiO^-, the mobility of EOF is negligible. In a buffer system, the net charge and the electrophoretic mobility are pH dependent [29] [30]. The electrolyte ionised at different pH, and each electrolyte behaves differently. For a high efficiency separation, the pH must be optimized such that the mobility of the buffer matches the mobility of the analyte. Poor optimized pH system will results in a decrease in electrophoretic mobility and peaks can be asymmetrical.

The material of the capillary affects the mobility of the buffer at different pH [20]-[24]. Figure 1.12 shows that Telfon and Pyrex are not suitable for pH lower than 4, while silica can be used from pH 2.5-8.

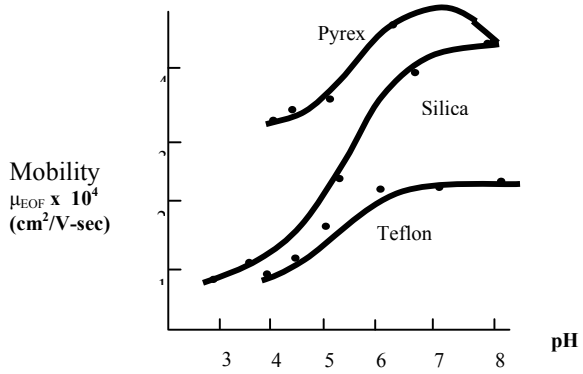

Figure 1.12: Effect of pH vs. EOF using different capillary materials. [20]

1.5.3 Buffer concentration

For a temperature controlled system, an increase inbuffer concentration (ionic strength) compresses the double layer due to a lower zeta potential resulting in a lower EOF. For a system without the temperature controlled system, at a given applied voltage, the increase of buffer concentration increases the current and hence the temperature, causing a decrease in the viscosity resulting in a higher EOF [20]. However, the incapability to dissipate heat will cause higher noise and baseline shift [30]. At low ionic strength, noise level can be lowered. However, at lower ionic strength, the peak efficiency decreases for a highly concentrated sample [30]. The ratio of the sample concentration to the carrier electrolyte concentration must be closely matched in order to achieve a high-resolution separation. Thus, the analysis of dilute samples, higher efficiency can be attained by using lower ionic strength buffer system.

1.5.4 Type of electrolyte

Different types of electrolyteswould cause different behaviour towards the overall buffer system. The interaction of analyte, wall of capillary, heat generated, EOF and the mobility of the ion [20] are the factors to be considered in setting up a new system. Well-established non-aqueous media was used for application of acidic drugs, dyes, preservative and even surfactants [30]. Aqueous buffer system remains popular in CE, for the easy preparation and handling [10]-[19],[25]-[29].

1.5.5 Organic solvent

Different solvent and the amount added to the buffer system will affect the viscosity of the buffer system. Since $\mu_{EOF} = \delta e/ \eta$ (4). With the addition of methanol to water, the viscosity increases up to 50% methanol then decreases subsequently. The addition of acetonitrile to water, the viscosity decreases from 0 to 100% acetonitrile [33]. Studies have shown that the addition of organic solvents such as methanol, ethanol, acetonitrile will increase the migration time and resolved mixtures of surfactants [33]. However, in other cases, there is no consistent correlation of the buffer viscosity to the behaviour of the EOF when adding organic solvents.

1.6 Modes of Injection

The more common methods of sample introduction into the capillary are by hydrodynamic and electrokinetic injection. In the following section, the basic principle of each injection method and the calculation of the volume injected are discussed.

1.6.1 Hydrodynamic injection

Sample introduction by hydrodynamic method means that the sample is injected by pressure at the inlet or by vacuum at the outlet (Figure 1.13). The pressure or vacuum and total time applied determines the sample volumes. Moreover, it is a function of the diameter and length of the capillary and the viscosity of the sample according to Hagen-Poiseuille equation [22][24] (9).

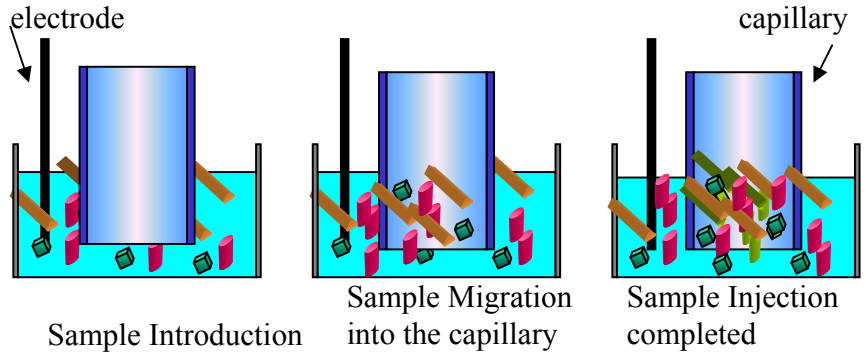

Figure 1.13: Hydrodynamic Injection model.

$$Vol = \frac{\Delta P \pi d^4 t}{128 \eta L_t} \qquad (9)$$

where,

ΔP = Pressure difference

d = ID of capillary

t = Injection time

η = Sample viscosity

L_t = Total Length of capillary

V = Sample volume

For example, an aqueous sample (η=0.1 Nsec/cm^2 for water) was injected for 5 seconds into a capillary of 50 μm ID and total length of 40 cm, at a pressure difference of 25 mbar, will be computed to have an injected volume as low as 8nL.

1.6.2 Electrokinetic injection

In electrokinetic injection, the capillary is dipped into the sample and a voltage is applied between the ends of a capillary. The quantity injected is dependent on the electrophoretic mobility of the individual solute (10). The conductivity of the sample is also a contribution factor to the sample loading. However, if a mixture contains a large quantity of one type of ions, over-loading of this ion will occur.

$$\text{Mole (mol or g) Injected} = (\mu_{EOF} + \mu_{EP})\, E\, (K_b/K_s)\, t\, \pi\, r^2\, C \qquad (10)$$

where,

μ = apparent Mobility of analyte

E = Applied Electric Field

(K_b/K_s) = Ratio of conductivites of buffer and sample

t = time

r = radius

C = concentration

1.6.3 Comparison of hydrodynamic and electrokinetic injection

Hydrodynamic injection has no discrimination of sample due to same ion mobilities, whether it is a higher charge or smaller size ion. However, it cannot be used in gel-filled capillaries, where the viscosity of the sample is too high, not allowing its flow by pressure provided by the CE system. Electrokinetic injection has discrimination i.e. injecting larger amounts of more mobile, smaller size samples relative to the slower, larger ions. Figure 1.14 shows the discrimination of an electrokinetic injection. The last peak of the sample is of lower charge compared to the first few peaks. Hence, electrokinetic injection is generally less reproducible as compared to hydrodynamic injection. This discrimination can be corrected with the additional of a known standard as an internal standard [18]. On the other hand, electrokinetic injection is advantage for the analysis of viscous or gels samples, where hydrodynamic injection is limited. The analytes enter the capillary by migration and pushing force by EOF, thus, electrokinetic injection is potentially a more sensitive method. The detection limits are greatly improved in several studies [34],[35] showing that the electrokinetic injection (ppt or sub-ppb) has trace enrichment behaviour as compare to sample injection by pressure (ppm) [36] [37].

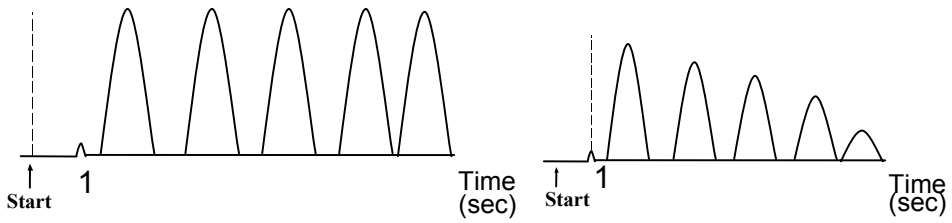

Figure 1.14A: Hydrodynamic injection showing no bias.

Figure 1.14B: Electrokinetic injection showing discrimination at the last peaks.

1.7 Sample Preconcentration

On-column sample concentration is a powerful alternative preconcentration method to improve the detection limit without long and tedious extraction methods.

1.7.1 Stacking

Simple stacking means the sample in a matrix has a higher resistance or a lower conductivity of the background solution. The greater the difference in conductivity or resistively the greater the concentrating effect. Therefore, a plug of water or organic solvent is injected onto the capillary filled with relatively high ionic strength operating buffer. The plug reduces the electric field between the sample zone and the electrolyte. The steeper the drop of electric field, the higher the enrichment. Large-volume sample stacking exploits the large difference in the resistively of the water zone and the analytes to pre-concentrate the sample up to 100 to 500-fold [38]-[40].

1.7.2 Transient isotachophoresis

In this on-line pre-concentration technique, the sample is introduced at the interface of a discontinuous buffer system, consisting of a leading (L) and a terminating (T) electrolyte. This technique is not as popular as stacking as more than one buffer system are required.

1.7.3 Electrostacking

Electrostacking pre-concentration technique comprised of transient isotachophoretic and electrophoretic separation. During electrokinetic injection, a lower ionic strength sample is 'stacked' between the lower field strength buffer and the sample zone (Figure 1.15). An isotachophoretic-terminating ion is usually added to the buffer and the sample to normalize the conductance. This terminating ion must be slower than the analyte so that it will not disturb the stacking or separation process [41].

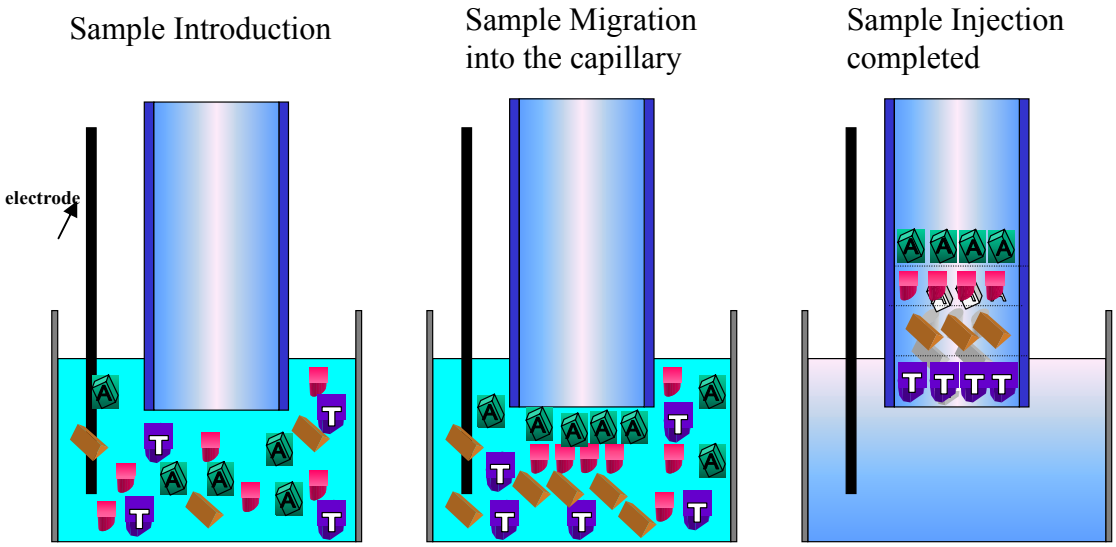

Figure 1.15: A schematic diagram to demonstrate a transient isotachophoretic preconcentration of sample during electrokinetic injection.

1.7.4 Sweeping

Sweeping is defined as the migration of a reagent such as a sodium dodecyl sulphate (SDS) micelle, which serves to bind the solutes and concentrate them in a narrow band [42]-[44]. In other words, the accumulating of the analyte molecules by pseudo-stationary

phase enters and fills the sample zone upon the application of voltage. The longer the analyte stays in the pseudo-stationary phase, the greater the pre-concentrating effect. This technique is applied in MEKC (section 1.7.3). Several studies on combining two or more pre-concentration techniques are applied to increase the detection limit to 100 000 fold [45]-[48].

1.8 Design of Experiment

The design of experiment (DOE) to determine certain main effects of a process or method is to measure some control factors and analysis the data set by statistical methods that were previously designed by mathematician. This designed experiment demonstrated the possibility to extract a large fraction of the information in a matrix from a smaller fraction in that matrix [54]. They are much more efficient than the traditional one-factor-at-a-time (1-FAT) method since the numbers of tests are minimize substantially. The large amounts of results from the 1-FAT method are hard to interpret and might even be misleading. Therefore, DOE is a simple way to save time and cost by reducing the number of experiments and still remain effective in evaluating a complex or unfamiliar process or method. The advancement in computer statistical software enables faster data processing and able to have appropriate graphical presentation. Several methods such as Interferential procedures, Analysis of Variance (ANOVA) technique, Fractional Factorial Designs (FFD), Orthogonal Array Designs (OAD), Surface Response and Taguchi method are available. The appropriate method for the DOE depends of complexity of the process/product.

1.8.1 Taguchi Methodology

Designed experiments by the methodology of Genichi Taguchi have been accepted in many Japanese companies [55][56] to characterize and optimize complicated multi-response processes with minimum numbers of experiments. The reduction of time-consuming tests not only increases the testing cycle time, but also saved on cost and wasted materials [57]. Taguchi used a systematic statistical approach to design experiments for robust products or processes [58]. It is based on quality engineering principles where experiments are on the product or process design rather than the process operation [59]. Therefore, when dealing with simultaneous optimization of more than one response in the same process, it required 'engineering judgements' on the confirmation results.

1.8.2 Design Structures

Taguchi determines factors that have effect on the product or process based on three design stages. They are 'System Design', 'Parameter Design' and 'Tolerance Design'. 'System Design is the primary design for developing a new product or new process. The key element of Taguchi approach is 'Parameter Design', the secondary design which determine the process parameters on factor levels such that the process is optimized and has minimum sensitivity to environmental factor, "noise" [62]. Lastly, 'Tolerance Design' is the tertiary design that determines the optimum tolerance settings of the product or process parameter with high quality improvement at a low cost.

Taguchi's design is based on the Fractional Factorial concepts with orthogonal array that allows multi-factor investigation. Besides, it is able to determine the main effects of two factors interaction. At the start of Taguchi array, the number of controllable and uncontrollable factors, number of levels of each factor must be known. The selection of these factors may require prior knowledge of the product or process. Taguchi adopts a 1, 2 system with 1 referring low and 2 means high level. The smaller the orthogonal array the shorter the experiment, hence reducing experimental costs. Some example of such small arrays are $\boldsymbol{L_4(2^3)}$, $\boldsymbol{L_8(2^7)}$ (Table 1.4) and $\boldsymbol{L_9(3^4)}$ arrays (Table 1.4). Other randomized run order arrays include $\boldsymbol{L_{16}(4^5)}$, $\boldsymbol{L_{18}(3^7)}$ and $\boldsymbol{L_{27}(3^{13})}$ arrays.

$\boldsymbol{L_9(3^4)}$				$\boldsymbol{L_8(2^7)}$						
1	2	3	4	1	2	3	4	5	6	7
1	1	1	1	1	1	1	1	1	1	1
1	2	2	2	1	1	1	2	2	2	2
1	3	3	3	1	2	2	1	1	2	2
2	1	2	3	1	2	2	2	2	1	1
2	2	3	1	2	1	2	1	2	1	2
2	3	1	2	2	1	2	2	1	2	1
3	1	3	2	2	2	1	1	2	2	1
3	2	1	3	2	2	1	2	1	1	2
3	3	2	1							

Table 1.4: Taguchi's $\boldsymbol{L_9(2^4)}$ and $\boldsymbol{L_8(2^7)}$ arrays.
$\boldsymbol{L_9(3^4)}$ has 9 experiments with 4 factors at 3 levels. $\boldsymbol{L_8(2^7)}$ has 8 experiments with 7 factors at 2 levels.

1.8.3 Performance Statistics

In contrast with classical statistical experiment, the response optimization or influences factors are determined not only on the average response but also on the signal-to-noise ratio (S/N) [61]. In this way, the mean level of the process (signal) and the variation around this mean (noise) are monitored as S/N. Contribution of factors assigned to the inner array of the orthogonal array is considered as signal, and all other factors are considered as noise factors. Therefore, each combination of control factor produces a S/N. Based on Taguchi's loss function each quality criterion, there are basically three S/N ratio [61],[63]:

1) S/N for larger the better (LTB) is calculated by (11) where Y_i - is raw data corresponding to this control factors combination, n - number of Y_i (number of experiments carried out at this control factors combination).

$$\text{S/N} = -10 \cdot \log\, 1/n \cdot \sum_{i=1}^{n} 1/y_i^2 \tag{11}$$

2) S/N for smaller the better (STB) is calculated by (12).

$$\text{S/N} = -10 \cdot \log\left[1/n \cdot \sum_{i=1}^{n} y_i^2\right] \tag{12}$$

3) In order to calculate S/N for nominal the best I as in (15), sensitivity (S_m) and sample variation (V_e) are calculated in (13) and (14) respectively.

$$S_m = \frac{1}{n} \cdot \left[\sum_{i=1}^{n} y_i \right]^2 \tag{13}$$

$$V_e = \frac{1}{n} \cdot \sum_{i=1}^{n} (y_i - \bar{y})^2 \tag{14}$$

$$\text{S/N} \quad = 10 \cdot \log\left[(S_m - V_e)/(n \cdot V_e) \right] \tag{15}$$

The S/N value for each response factor is calculated from the individual response factor.

1.8.4 Data Plots

The data plots are graphical data to show the mean of each performance response and factor influences, called main effect plots. The higher end-point of the line shows the optimal level. It is ideal for all optimal factors to be shown in all responses. Sometimes, there are conflicts where one optimal level occurs in one response but not another. In that case, it is required 'engineering' perception or 'trade-off' performance for an optimized condition for all responses. The following case study is to illustrate the interpretation of the data plot of a simple experiment of emission of carbon monoxide (CO) [58]. A Taguchi matrix with 7 factors 2 levels, $\boldsymbol{L_8}$, was designed by determined with one response, i.e. the minimum emission of CO. Figure 1.16 showed the S/N ratio plot and the mean plot. From the S/N plot, the main factors of the greatest effect of the process were D and E. Both plots had a downward trend as tested level increased. The less significant factors were A, B, C and F. Only G appeared to have least influence on S/N. The level for G was chosen depending on other factors such as lower cost. Thus, for the

maximum S/N ratio, the optimal combinations would be A1, B1, C2, D1, E1, F2 and G1. The mean plots shown a similar overall factors effect as S/N plots. Since the experiment was based on the minimum CO, the optimal combination would be A1, B1, C2, D1, E1, F2 and G1.

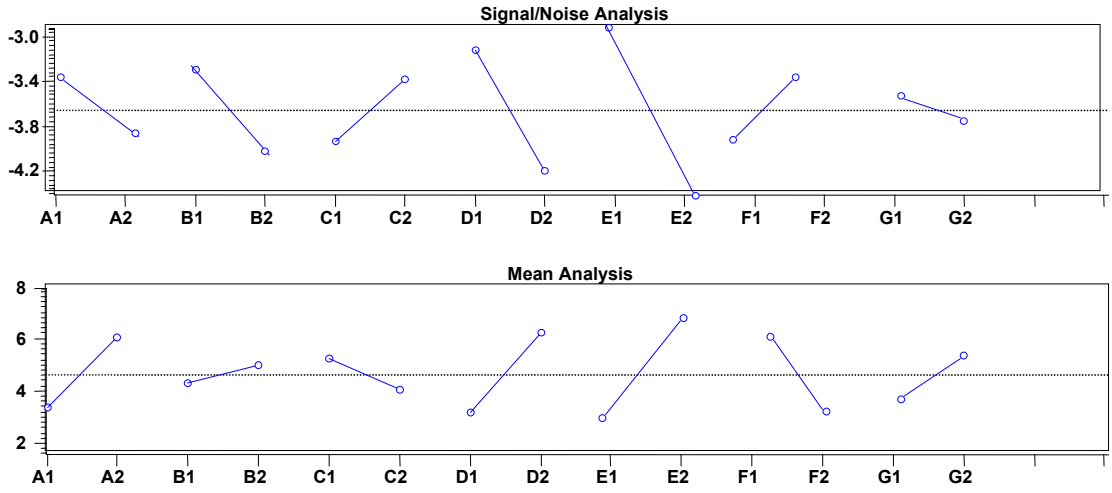

Figure 16: An illustration of a S/N and mean data plots.
(The S/N and mean plots for CO emission experiment.)

The overall factor effect for both S/N and mean were the same, where D and E showed the main effecting factors and the optimal combination was A1, B1, C2, D1, E1, F2 and G1.

1.8.5 ANOVA Modeling

After the analysis of effect, the screening design based on ANOVA principle are carried out to assessed and confirm the statistical significance of the effects factors. ANOVA is based on splitting the response variation, S (16), and the total sum of squares, St, into

sum of squares corresponding to the important effect, S'. The response variance, V, is the conversion of variation to variances based on the number of degree of freedom (18). The variance ratio, F, is the variance of main effect response to the variance of least effect response (19). ANOVA table illustrated the sum of square in term of ρ *(%)* (20). If ρ *(%)* is > 5, the factor is highly significant.

$$S = \sum y_i^2 - (\sum y_i)^2 \quad (16)$$

$$S' = S - Ve \cdot f \quad (17)$$

where,

f = degree of freedom
Ve = variance of least effect response

$$V = S / f \quad (18)$$

$$F = V / Ve \quad (19)$$

$$\rho\ (\%) = S' / St \cdot 100 \quad (20)$$

1.9 Scope of project

There were many literatures on the analysis of surfactant especially in the commercial products and environmental studies [65]-[67]. A routine application for the determination of trace analysis of anionic surfactant on silicon wafer that is required to meet the demand of high purity wafer surface in semiconductor industry is absent. The presence of high-level fluoride ions and silicon ions matrix [68] is the key problems to the determination of ultra trace anionic surfactant concentration. Capillary electrophoresis (CE) is widely recognized as a separation technique with many advantages to other techniques, such as high efficiency, fast separation, low consumption of chemical reagents, and most importantly small sample size needed for one analysis. The primary objective of this project is to develop a method for the analysis of surfactants, where the main active agent contains dodecylbenzene sulfonate (DBS), by CE. It is to explore the feasibility developing of a robust and trace analysis method for DBS on wafer surfaces in a complicated sample matrix containing high concentration of hydrofluoric acid (HF). Many factors that affect the buffer systems, which include the voltage, pH, type of buffer and its concentration, and modifiers, are scrutinized to determine the main effecting parameters. In order to achieve ultra trace analysis, pre-concentration of the sample as well as the uses of different mode of injection methods are evaluated to obtain an optimized system.

All of these parameters are very often required in a great number of laboratory analytical experiment that are tedious and at high laboratory cost if one factor is changed at one

time. A systematic design of experiment will be effective to investigate these parameters at a reduced number of experiments. Taguchi methodology is adapted systematically in developing a analysis of DBS on silicon wafer surface by CE.

In this chapter, two major topics are disccussed. Firstly, the basic principle of capillary electrophoresis and the different mechanism of separations available were discussed. The factors that can be varied to achieve desirable separation performance are also mentioned. Secondly, the design of experiment based on Taguchi methodology is discussed. Taguchi designs matrix structures (L_4, L_8, L_9 etc) to allow experimenter to evaluate the parameters and levels and determined the main effect easily and systematically. Since the design matrix was based on statistical orthogonal array, the number experiment was reduced sufficiently. The data plots and ANOVA table help to evaluate the results simply and logically without the need to go through the traditionally tedious statistical calculations.

In this study, two sets of experiment will be investigated. First is the determination of a robust buffer system for the analysis of dodecylbeneze sulfonates (DBS). A L_{18} design matrix was created based on 1 factor at 2 levels, and 7 factors at 3 levels. The factors include the type of electrolyte, and its concentration, pH, voltage and modifiers like as organic solvent, SDS and CDs. This matrix was superimposed by a noise factor of hydrofluoric acid at 5 levels. This experiment was repeated three times for better statistical results. Hence, 270 data will be generated for each response. The sensitivity of DBS peaks were evaluated. In ‘all-in-one’ analysis, the higher the corrected peak areas of single DBS peak, the better the sensitivity. In ‘fingerprint' analysis, the greater

number of well-separated DBS peaks, the better the quality of analysis. Other responses, the number of peaks and corrected peak area, the symmetry and the migration were monitored and evaluated.

Second, lowering the detection limit of the optimized 'all-in-one' buffer system will be carried out. Again, a Taguchi design structure, $\boldsymbol{L_{16}}$ matrix was created based on 4 factors at 4 levels, and 3 factors at 2 levels. The factors include injection time, sample pre-concentration by different solvents and quantity inject before sample, voltage ramp up rate, flushing of buffer before and after injection,the mode of injections and post-conditioning. Here, only the corrected peak of the single DBS peak was monitored. The larger the peak area, the better the sensitivity.

2. Experimental

2.1 Clean room Environment

The clean room standard in the wafer manufacturing industry was closely controlled with regular audit under International Organization for Standardization (ISO), ISO 14644-1, entitled "Cleanrooms and associated controlled environments - Part 1: Classification of air cleanliness." ISO Class 4 (Class 10 in Federal Standard 209 E). This means that the maximum concentration of air particles does not exceed 10 000 particles of size equal to or larger than 0.1 μm per cubic meter (m^3) in a laminar flow system. In order to maintain the quality of the sample and testing solution, all experiments were carried out in a ISO Class 4 clean room.

2.2 Reagents

All chemicals were purchased from Aldrich and Merck and were of analytical grade or better. The ultra pure water (UPW) fulfilled the requirement of the SEMI F61-0301 guidelines for pure water in semiconductor processing [64], i.e. cationic contamination smaller than 5 ng/L and anionic contamination smaller than 20 ng/L. Dodecylbenzene sulfonate (DBS) sodium salt was obtained from Fluka, Germany. Quality control (QC) standard DBS standard was obtained from Aldrich, USA. All buffer solutions and standards were prepared daily in cleanroom of ISO Class 4 (ISO 14644-1). The pH values of all prepared buffer solutions were measured with a daily calibrated pH meter (Mettler Toledo M235).

2.3 Instrumentation and Software

2.3.1 HP^{3D}CE

The instrument used in this project is HP^{3D}CE from Agilent Technologies (Waldbronn, Germany) set at a constant temperature of 20°C. Fused silica capillaries (50µm internal diameter, ID and 350µm OD) were obtained from Polymicro Technologies (Phoenix, AZ, USA). The length used in this experiment was 64.5cm (56 cm to the detection window). Detection wavelength was at 200 nm and 194 nm with a bandwidth of 10 nm and 6 nm respectively.

2.3.2 ChemStation software for HP ^{3D}CE

ChemStation software controls the instrument with very simple graphical user interface (GUI) systems or shortcut icons. The basic structure of this software consists of three main components: 1) Instrument Control, 2) Methods and Sequences and 3) Data Analysis.

2.3.2.1 Instrument control

In GUI system, the actions were reflected in a graphically manner as shown in Figure 2.1. Some of the main actions include switching the lamp on, start of an analysis, controlling the sample tray, applying voltage or pressure across the samples etc, by simply clicking

in the icons. The ‘On-line’ and ‘Off-line’ instrument Control allowed the user to quantify the result, edit methods and evaluate data while the instrument was at ‘analysis’ mode.

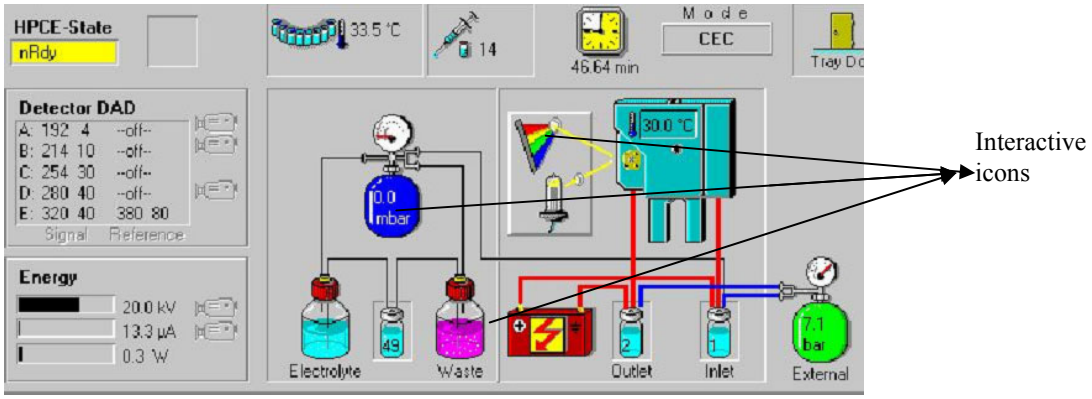

Figure 2.1: Interactive Chemstation software.

The GUI shows the action of external pressure and voltage across the sample vials 2 and 3.

2.3.2.2 Methods and sequences

In a ‘Method’, a series of actions were instructed to carry out for each analysis. The ‘Method’ set up interface consists of three sections. Firstly, the method allows setting the conditioning and temperature of the capillary, and replishment of buffer. Secondly, the method allows the injection of sample either by pressure or voltage. Lastly, the selection of wavelength of the diode arrays detector (DAD).

In a ‘Sequence’, a list of samples was created. This ‘Sequence’ was created to automate the analysis for several samples. The ‘Sequence Table’ determines the method to be used, the position for the sample, and the order of analysis. During the entire analysis process,

the HP ChemStation tracked the sequence's progress in real time and produced a sequence batch log file.

2.3.2.3 Data analysis

In Data Acquisition, all signals are converted from analogue signals to digital signals. The digital signal was transmitted to the HP ChemStation electronically and stored in the signal data file. During integration, the software identified a start and end time, the apex and the migration time for each peak. Then, the area, height, and peak width for each peak were calculated. By entering the concentrations and the concentration levels of the samples, a calibration curve was created. External standard calibration (ESTD) or internal standard calibration (ISTD) can be used. Usually, hydrodynamic injection mode used ESTD calibration while electrokinetic injection mode used ISTD calibration. ISTD can correct any variation caused by discrimination during electrokinetic injection, (see section 1.5.3).

2.3.3 Taguchi Software

ANOVA-^{TM} for windows was the software for generating the Analysis of Variance (ANOVA) tables based on Taguchi methodology [63]. This statistical tool can analyze the following as listed in [60][61]:

- Variable and Attribute Data Analysis
- Signal-to-Noise Ratio Analysis
- Sensitivity Analysis
- Dynamic Characteristics
- Confirmation Runs
- Combination and Idle Column Design
- Dummy Treatments
- Support for up to three outer arrays

A combination column design was generated when the parameters and levels were entered into the software. An example of a modified $\boldsymbol{L_{18}}$ layout for 1 parameter 2 levels (2^1) and 7 parameters 3 levels (3^7) and modified $\boldsymbol{L_{16}}$ layout for 4 parameter 4 levels (4^4) and 2 parameter 2 levels (2^2) are shown in Table 2.1 and 2.3. The number of experiments were carried out according to the test matrix. After the completion of the all experiments, all the data were entered into the Data column. ANOVA table, tables and graphs based on the mean, S/N or sensitivity will be generated. The advantage of ANOVA over other statistical tool was the ability to compute a projected mean and the S/N values when the

optimized parameters and levels were entered. The projected mean and S/N values changed as the selection of the parameters and levels changes. However, it was mandatory to run a confirmation run to make sure the selected parameters were practical to apply in daily analysis.

2.4 Design Parameters for DBS by CE

Many works have been done on the parameters influencing separation and detection of anions by CE [21]. The main parameters affecting the performance of a buffer system for the optimum separation of the analytes and overall stability of the system were the type of electrolyte, electrolyte concentration, pH and additive solvents or complexing additives.

2.4.1 Type of electrolyte and concentration

Phosphate and borate buffers were commonly and successfully used as electrolytes for the separation of alkyl benzene sulfonates [10]-[12]. Both phosphate and borate differed in their buffering range, their affinity to the capillary wall and their contribution to Joule heating. The increase of buffer concentration leads to increased migration time and peak resolution of the DBS isomers due the higher ionic strength. However, as the ionic strength of the buffer increased, the Joule heating increases due to the inability to dissipate heat at a high current.

2.4.2 pH

The pH value affected the mobility of the electroosmotic flow and thus the resolution of mixtures of anionic surfactants. At lower pH (4-5), the EOF was suppressed, causing minimum movement of the buffer. In the separation under reverse EOF, at higher pH (8-9) the mobility of EOF was higher, thus help to increase the migration time.

2.4.3 Organic solvent modifier

Organic solvent was added to modify the resolution of mixtures of surfactants because the micelle formation and the interaction between surfactant molecules were reduced suppressed. The degree of influence depended on the type of solvent [20]. Organic solvent added to the buffer also reduced the mobility of EOF, increased peak resolution and conductivity of the buffer, and decreased Joule heating but showed a higher tendency of bubble formation within the capillary while applying high electrical fields due to increase volatility.

2.4.4 Organic solvent concentration

The solvent concentration affected not only the micelle formation of the analyte surfactant but also micelle formation of separation surfactant – sodium dodecylsulfate (SDS). SDS, an anionic non-chromophoric surfactant, was added to the buffer in order to introduce an interaction between the alkyl chains of the analyte surfactant and the micelle improving peak resolution.

2.3.5 Surfactant modifier

Anionic analyte surfactant preferred to interact with SDS than the solvent, which was called *solvophobic* association [22]. Different lengths of hydrophobic alkyl chain to the phenyl ring forms associate complexes of different hydrophobicities, resulting in different electrophoretic mobilities causing good separation of isomers of DBS homologs. The lower the concentration of the organic solvent, the association between the SDS monomer and the anionic surfactant was more preferred [22]. Thus interaction helped to improve peak resolution.

2.3.6 Cyclodextrin modifier

Cyclodextrin (CD) was used as a chiral selector to improve the peak resolution by enhancing selectivity. The pure isomer homologs of DBS were resolved due to the formation of inclusion host-guest complexes with DBS molecules. The long alkyl chain could interact with the small hydrophobic cavity of α-CD, while the aromatic ring could interact with the larger cavity of β-CD. The neutral CD migrates with the EOF while the anionic surfactant experiences increased mobility towards the cathode. The use of CDs was reported to reduce/disrupt surfactant aggregate or micellization in the buffer system and capillary surface [8].

2.5 Design of Experiment by Taguchi Methodology

2.5.1 Test matrix for screening parameters of DBS- $\boldsymbol{L_{18}}$ layout

The factors affecting the analysis of DBS was shown in Table 2.1, 1 factor at 2 levels and 7 factors at 3 levels. A modified $\boldsymbol{L_{18}}$ layout matrix in Taguchi methodology was established is shown in Table 2.2. $\boldsymbol{L_{18}}$ layout consisted of 18 experiments with combination of factors and their levels. For example, Experiment 1: 25 mmol/L phosphate buffer system at pH 7.0 was prepared without any organic solvent, SDS and CD. DBS standard was analysed at 15 kV electrical field. The sample used here was 250 µmol/L of DBS. Hydrofluoric acid (HF) was added into the sample at 4 different concentrations, 0.50 µmol/L, 1.0 µmol/L, 5.0 µmol/L and 10 µmol/L respectively. 5 sets of 18 experiments with 3 replicates (5 X 3 X 18) would generate 270 data.

For analysis of the 'fingerprint' of DBS, the following list is the responses monitored, S/N equation used:

- Number of peaks – larger the better (LTB)- better separation.
- Corrected peak area – larger the better (LTB)- higher sensitivity.
- Symmetry of (last) peak – nominal the best I - overloading the buffer system.
- Migration time of (last) peak – smaller the better (STB)- faster separation.

For analysis of the 'one peak' of DBS, the responses monitored were similar to 'fingerprint' analysis, only the number peak was smaller the better (STB):

- Number of peaks – smaller the better (STB)- higher sensitivity.

2.5.2 Test matrix for optimization of DBS ultra trace analysis- L_{16} layout

A list of parameters that would increase the sensitivity of DBS is shown in Table 2.3. 16 experiments were designed according to the 4 levels 4 factors and 2 levels 3 factors together with 5 levels of HF as 'noise'. A modified L_{16} layout matrix is as shown in Table 2.4. For example, in Experiment 1: 2 min flushing of buffer during precondition where no post conditioning was required. 5 sec of water plug was injected before the DBS standard was injected hydrodynamically for 10 sec. The voltage was ramp up to 30 kV at a rate of 0.1 min per kV. The total number of data with 3 replicates resulting in a total of (5 X 3 X 16) 240 were generated. The sample used here was 5 μmol/L of DBS. The HF concentration was the same for L_{18} layout. The peak area was the only response that was monitored. The S/N equation used was larger the better (LTB). The larger the peak area observed, the higher the sensitivity, therefore a better performance of the analysis.

Noise matrix c(HF) [mmol/L]	0	0.5	1	5	10

Parameter	Factor Name	Level		
		1	2	3
A	type of electrolyte	phosphate	borate	
B	conc. of electrolyte [mmol/L]	25	50	75
C	pH	7.0	8.0	9.0
D	type of organic solvent	acetonitrile	methanol	THF
E	conc. of solvent [%]	0	10	25
F	conc. of SDS [mmol/L]	0	25	50
G	electrical field [kV]	15	22.5	30
H	cyclodextrin	0	10 alpha	20 beta

Table 2.1: List of Factors / Levels for the screening evaluation of parameter of DBS.

Group	A	B	C	D	E	F	G	H
Exp								
1	1	1	1	1	1	1	1	1
2	1	1	2	2	2	2	2	2
3	1	1	3	3	3	3	3	3
4	1	2	1	1	2	2	3	3
5	1	2	2	2	3	3	1	1
6	1	2	3	3	1	1	2	2
7	1	3	1	2	1	3	2	3
8	1	3	2	3	2	1	3	1
9	1	3	3	1	3	2	1	2
10	2	1	1	3	3	2	2	1
11	2	1	2	1	1	3	3	2
12	2	1	3	2	2	1	1	3
13	2	2	1	2	3	1	3	2
14	2	2	2	3	1	2	1	3
15	2	2	3	1	2	3	2	1
16	2	3	1	3	2	3	1	2
17	2	3	2	1	3	1	2	3
18	2	3	3	2	1	2	3	1

Table 2.2: Taguchi Matrix; Modified $\boldsymbol{L_{18}}$ layout ($2^1\ 3^7$).

Noise matrix c(HF) [mmol/L]	0	0.5	1	5	10

Parameter		Level			
		1	2	3	4
A	Injection Time	10	20	30	40
B	type of solvent before sample	water	methanol	Acetonitrile	acetone
C	plug length before sample [sec]	5	10	15	20
D	voltage ramp [min]	0.1	0.5	1	2
E	buffer flushing [min]	2	6		
F	mode of injection	hydrodynamic	electrokinetic @-5kV		
G	water flush post condition	0	3		

Table 2.3: Factors and levels for the Optimization of ultra-trace analysis of DBS.

Group	A	B	C	D	E	F	G
Exp							
1	1	1	1	1	1	1	1
2	1	2	2	2	1	2	2
3	1	3	3	3	2	1	2
4	1	4	4	4	2	2	1
5	2	1	2	3	2	2	1
6	2	2	1	4	2	1	2
7	2	3	4	1	1	2	2
8	2	4	3	2	1	1	1
8	3	1	3	4	1	2	2
9	3	2	4	3	1	1	1
10	3	3	1	2	2	2	1
11	3	4	2	1	2	1	2
12	4	1	4	2	2	1	2
13	4	2	3	1	2	2	1
14	4	3	2	4	1	1	1
15	4	4	1	3	1	2	2

Table 2.4: Taguchi Matrix; Modified $\boldsymbol{L_{16}}$-layout ($4^4\ 2^3$)

2.6 Procedure of Buffer and Standards preparation

Phosphate and borate buffer systems at pH 7, 8 and 9 were prepared, Table 2.5. For example, 25 mmol/L phosphate buffer at pH 7 was prepared with concentration of sodium dihydrogen phosphate (NaH_2PO_4) 10.75 mmol/L and concentration of disodium hydrogen phosphate (Na_2HPO_4) 14.25mmol/L. All self-prepared buffers were filtered (0.45 µm pore diameter) and degassed in an ultrasonic bath (30min) prior to use. The conditioning of new capillary was done as according to [19].

phosphate			
	25 mmol/L	50 mmol/L	75 mmol/L
pH 7	c(NaH2PO4) = 10.75 mmol/L c(Na2HPO4) = 14.25 mmol/L	c(NaH2PO4) = 21.5 mmol/L c(Na2HPO4) = 28.5 mmol/L	c(NaH2PO4) = 32.25 mmol/L c(Na2HPO4) = 42.75 mmol/L
pH 8	c(NaH2PO4) = 1.7 mmol/L] c(Na2HPO4) = 23.3 mmol/L	c(NaH2PO4) = 3.4 mmol/L c(Na2HPO4) = 46.6 mmol/L	c(NaH2PO4) = 5.1 mmol/L c(Na2HPO4) = 69.9 mmol/L
pH 9	c(NaH2PO4) = 0.1 mmol/L c(Na2HPO4) = 24.9 mmol/L	c(NaH2PO4) = 0.2 mmol/L c(Na2HPO4) = 49.8 mmol/L	c(NaH2PO4) = 0.3 mmol/L c(Na2HPO4) = 74.7 mmol/L
borate			
	25 mmol/L	50 mmol/L	75 mmol/L
pH 7	c(Na2B4O7) = 0.1 mmol/L c(H3BO3) = 24.9 mmol/L	c(Na2B4O7) = 0.2 mmol/L c(H3BO3) = 49.8 mmol/L	c(Na2B4O7) = 0.3 mmol/L c(H3BO3) = 74.7 mmol/L
pH 8	c(Na2B4O7) = 0.875 mmol/L c(H3BO3) = 24.125 mmol/L	c(Na2B4O7) = 1.75 mmol/L c(H3BO3) = 48.25 mmol/L	c(Na2B4O7) = 2.625 mmol/L c(H3BO3) = 72.375 mmol/L
pH 9	c(Na2B4O7) = 11 mmol/L c(H3BO3) = 14 mmol/L	c(Na2B4O7) = 22 mmol/L c(H3BO3) = 28 mmol/L	c(Na2B4O7) = 33 mmol/L c(H3BO3) = 42 mmol/L

Table 2.5: Preparation of phosphate and borate buffer systems.

The standard reference solutions of 250 µmol/L DBS were prepared daily by diluting from the stock solution. The stock solution of 10 mmol/L was made from the corresponding sodium salts, 1.36g of DBS to100 mL ultra pure water (UPW). A series of DBS standards of 0.025, 0.05, 0.10, 0.25, 0.50, 1.0, .5, 5.0, 10, 25, 50, 100, 150, µmol/L were diluted from 250 µmol/L. In every run, 900 µL of standard and 100 µL of

concentration of hydrofluoric acid (HF); 5 µmol/L, 10 µmol/L, 50 µmol/L, 100µmol/L, were pre-mixed in a vial. In spike recovery, 100 µL of 250 µmol/L (***L*** $_{18}$) and 50µmol/L (***L*** $_{16}$) were added to 800 µL standard and 100 µL of HF at the appropriate concentration.

2.7 Extraction procedure of Wafer Sample

Surfactant contaminants can be found on the oxide layer and within the native oxide film. Hydrofluoric acid fume was used to remove the native oxide film so that the surfactant can be dissolved totally by water.

2.7.1 Wafer sample extraction by manual swirling method

The surfactant from the 200-mm silicon wafer surface was extracted with 2-mL ultra pure water (UPW) completely wetting the surface and swivelling the wafer for 2 min. A sample of 900 µL was pipetted from the wafer surface. 100µL of c(HF) 10 µmol/L was added into the vial. For wafer recovery, another wafer from the same batch lot was intentionally contaminated with spiking solution: 1) 50 µmol/L DBS for ***L*** $_{18}$; 2) 5 µmol/L DBS for ***L*** $_{16}$, by completely wetting the surface with 2 mL of spiking solution. The wafer were dried in a cleanroom of class 4 (ISO 14644-1) for 2 hours. The sample was collected.

2.7.2 Wafer sample extraction by VPD-manual swirling

Vapour phase deposition (VPD)-manual method was similar to the non-VPD method (section 2.7.1), only difference was that the wafers were fumed in 49% ultra pure HF

chamber for one hour prior to collection of sample by swirling with 2 mL of UPW on the wafer surface [18]. It is assumed in dissolving the native oxide, the van-der-Waals interaction between polar compounds such as surfactants and the wafer surface was cancelled. The HF reacted with the 5-nm thickness of native layer of silicon wafer and 10 monolayers of a surface water film to form fluosilicic acid and water micro-droplets. All soluble contaminants, including surfactant, would be collect by scanning with 2 mL of UPW.

2.7.3 Wafer sample extraction by VPD-WSPS method

Wafer Sample Preparation System (WSPS) was designed to collect contamination on wafer surface by scanning the entire wafer surface by robot arm. The system was attached with a fume chamber to allow fully automation. Here, 100 µL UPW was used to scan the hydrophobic silicon surface after HF fumed for 10 min and 20 min. 2 mL of 0.5 µmol/L DBS (***L*$_{16}$** only) was intentionally spiked on the of the wafer surface for a recovery check of 10 µmol/L.

3. Results and Discussion

3.1 Part I- Screening of Parameters for DBS analysis based on L_{18} Layout

3.1.1 Systematic selection of Parameter for DBS buffer system

In Taguchi analysis, it was important to note that the higher the S/N the better the results. The Signal/Noise Analysis results for Area (mAU), Figure 3.1, showed clearly the factor C, F, G (i.e. C-plug length before sample; F-mode of injection; G-Electrical Field) were the main factors affecting the system. Factor-Level C3, F1 and G3 were the highest while C1, and F2 had the lowest value. Factor A, B, D, E and H were least effect on S/N for Area. Therefore the Factor-Levels were chosen according to easy process control, practicality and cost.

Other responses, such as migration time, would differ in the main factor affecting this response. Therefore, a set of compromised parameters for all four responses, i.e. area, migration time, symmetry, and number of peaks, were selected as ideal combination. As shown in Table 3.1,. the main effect factors were marked against it in individual responses. In the last column, overall choices would then be selected. The optimum parameter was first selected based on the highest S/N values for all the four responses (Table 3.4), and secondly by making use of the Taguchi software to predict the S/N values as a guide for the selection of parameters. Thus, the parameters were selected based on the highest predicted S/N values.

For the type of electrolyte, i.e. phosphate and borate, Factor-Levels A1 and A2 did not show significant effect on any of the responses. Factor-Level A2 (borate) showed slightly higher S/N value than phosphate (A2) for migration time. Considering peak symmetry, borate showed a better performance then phosphate. The sensitivity for symmetry was greatly improved if borate buffer system was used.

The highest ionic strength of the buffer, B3, had the highest sensitivity for symmetry, but also the least number of peaks resolved. The best choice was the medium ionic strength, B2, as most of the S/N values were high for all responses except for symmetry. However, the S/N values did not vary too much if the lowest ionic strength buffer, B1, was used. It will be practical to use a lower concentration buffer solution to minimize the potential problem caused by Joule heating. Furthermore, in order to have a closely match ratio of concentration of sample to ionic strength of buffer [30], for a lower concentrating sample, a lower concentration buffer system would be preferred. Therefore, B1 was selected.

Organic solvents were added to modify the resolution of mixtures of surfactants because the micelle formation and the interaction between surfactant molecules were reduced or suppressed [31]. The degree of influence depended on the type of solvent [20]**.** Organic solvent added to the electrolyte also reduced the mobility of EOF, increasing peak resolution and reduced conductivity of the electrolyte, thus decreasing Joule heat. But the addition of solvent into the electrolyte caused a higher tendency of bubble formation within the capillary while applying high electrical fields. Factor D, type of solvent,

improved the sensitivity for symmetry in D1. Peak area was the highest without adding any organic solvent, SDS and CD because DBS, which moved along with EOF, was not resolved in its homologues and isomers. For the "all-in-one" buffer system, the response criterion "Smaller the Better" regarding the number of peaks was adopted.

Factor F, concentration of SDS, had a major effect on the migration time (MT). Although there was an increase of MT in F1, the absence of SDS greatly reduced the number of peak in the 'fingerprint' DBS analysis system. To compromise, F2, 25 mmol/L of SDS would give an optimum number of peaks at reasonable migration. For the 'all-in-one' buffer system, F1 was chosen. Without any additives, a shorter analysis time was obtained shifting the isomers and homologues into nearly one peak and, thus, improving the sensitivity. Adding SDS and CD lengthens analysis time but with better resolution of the isomers and homologues. In the absence of organic solvent, SDS forms association complex with the hydrophobic dodecyl chain due to stronger solvophobic interaction, while the larger cavity β-CD forms inclusion complex with the aromatic ring of DBS resulting in a better resolution [14]. This offered some benefits for 'fingerprint' analysis. Thus, H3, 20 μmol/L beta CD was selected.

The best combination of Factor-Level after the analysis and simulation of S/N values were as follows:

(1) An optimized system for LAS (fingerprint) CE analysis, the 8 Factor-Levels were A2, B1,C3, D2, E1, F2, G3 and H3 (see Table 3.1);

(2) An optimized system for LAS (one peak) CE analysis, the 8 Factor-Levels were A2, B1, C3, D1, E1, F1, G3 and H1 (see Table 3.2).

Label	Factor Name	Choice Level
A2	type of electrolyte	borate
B1	conc. of electrolyte [mmol/L]	25
C3	pH	9.0
D2	type of organic solvent	-
E1	conc. of solvent [%]	0
F2	conc. of SDS [mmol/L]	25
G3	electrical field [-kV]	30
H3	cyclodextrin	20 beta

Table 3.1: Optimized system for Fingerprint analysis.
All peaks were detected by direct photometeric detection at 194 nm At a constant temperature of 20°C. Fused silica capillaries, 50µmm ID, a total length of 64.5cm (56 cm to the detection window).

Factor Name	Choice Level	
A2	type of electrolyte	borate
B1	conc. of electrolyte [mmol/L]	25
C3	pH	9.0
D1	type of organic	-
E1	conc. of solvent [%]	0
F1	conc. of SDS [mmol/L]	0
G3	electrical field [-kV]	30
H1	cyclodextrin	0

Table 3.2: Optimized system for One-peak analysis.
All peaks were detected by direct photometeric detection at 194 nm At a constant temperature of 20°C. Fused silica capillaries, 50µmm ID, a total length of 64.5cm (56 cm to the detection window).

	Area (mAU* sec)		Migration Time (min)		Symmetry		No. of Peaks	
	Mean	**S/N**	**Mean**	**S/N**	**Mean**	**S/N**	**Mean**	**S/N**
L_{18} Results	1.19	-2.49	20.76	-23.96	0.858	11.2	6.8	11.1
Prediction	2.91	13.5	9.78	-21.54	1.142	7.517	10.7	25.6
After Confirmation Run	**0.15**	**-16.5**	**10.82**	**-20.96**	**1.365**	**14.285**	**16**	**24**

Table 3.3: Tabulation of Mean and Signal-to-noise ratio for the L_{18} experiment.
For both the predicted values and the confirmation run for the 'fingerprint' analysis.

3.1.2 Confirmation run for L_{18} Experiment

Confirmation analyses were mandatory to validate the chosen parameters and the levels. The electrophoregrams for the 'confirmation' runs show a well separated peak and one single large profound peak in the 'fingerprint' and 'one peak' buffer system respectively (Figure 3.2, 3.3). There was also an absence of skewed peaks, the buffer systems were proven to be able to qualify and quantify the analysis of DBS (see Section 3.1.3). In Table 3.3, the predicted mean values were closed to the results of the actual run, especially for the number of peaks.

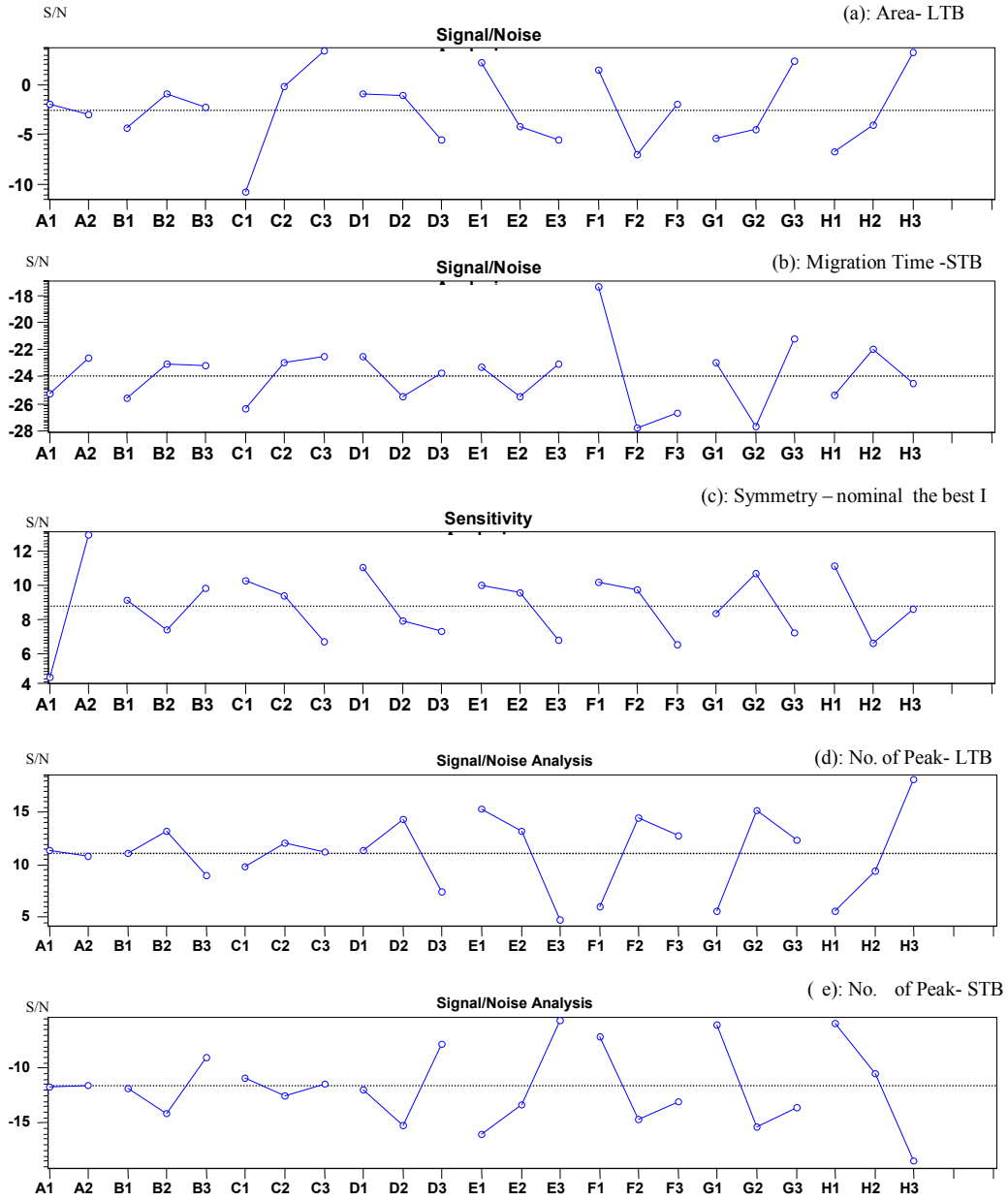

Figure 3.1: S/N result for the screening of parameters for DBS by ANOVA.

(a), (b) and (c) are response factor for Area, Migration Time and Symmetry. (d) and (e) are response factor for No of Peak, fingerprint analysis and single peak analysis respectively. ---- line represents the average S/N values.

A-type of electrolyte: phosphate, borate; B-conc. of electrolyte [mmol/L]: 25, 50, 75; C:- pH: 7.0, 8.0, 9.0; D-type of organic solvent: acetonitrile, methanol, THF; E- conc. of solvent [%]: 0, 10, 25; F- conc. of SDS [mmol/L]: 0, 25, 50: G- electrical field [kV]: 15, 22.5, 30; H- cyclodextrin: 0, 10 alpha, 20 beta. All peaks were detected by direct photometeric detection at 200 nm.

				Area		Area Choice	Migration Time (min)		MT Choice	Symmetry		Sym Choice	No. of Peaks		No. Peak Choice	Overall Choice
		Levels		Mean (mAU*sec)	S/N (dB)		Mean (min)	S/N (dB)		Mean	S/N (dB)		Mean ( )	S/N (dB)		
A	Type of electrolyte	1	phosphate	926.4	-1.9583		23.82	-25.25		0.515	12.591	1	8	11		
		2	borate	795.3	-3.0276		17.68	-22.66		1.201	9.761		5	11		**A2✓**
B	Conc. of electrolyte [mmol/L]	1	25	1,003.40	-4.2868		24.9	-25.61		0.946	4.678		6	11	1	**B1✓**
		2	50	826.5	-0.9481		17	-23.09		0.735	12.132		7	13		
		3	75	752.8	-2.2438		20.39	-23.17		0.893	16.718	3	7	9		
C	pH	1	7	499.3	-10.7628		29.22	-26.33		0.918	6.366		8	10		
		2	8	761.4	-0.2060		18.15	-22.98		0.9	11.292		7	12	2	
		3	9	1,321.90	3.4900	3	14.86	-22.56	3	0.756	15.87	3	4	11		**C3✓**
D	Type of organic solvent	1	Acetonitrile	804.9	-0.8442		15.61	-22.59		1.05	13.976		6	11		
		2	Methanol	940.4	-1.0992	2	27.08	-25.48		0.719	14.637	2	10	14	2	**D2✓**
		3	THF	837.3	-5.5354		19.67	-23.8		0.805	4.915		4	7		
E	conc. of solvent [%]	1	0	966.4	2.2311	1	20.27	-23.3	1	0.89	13.041		10	15	1	**E1✓**
		2	10	872.2	-4.1767		22.32	-25.46		0.84	13.418	2	8	13		
		3	25	744	-5.5331		19.7	-23.11		0.843	7.069		2	5		
F	Conc. of SDS [mmol/L]	1	0	523.3	1.5090	1	7.6	-17.34	1	0.946	12.058	1	2	6		
		2	25	734.3	-6.9853		28.68	-27.8		0.916	10.523		9	14	2	**F2✓**
		3	50	1,325.00	-2.0025		26.1	-26.74		0.713	10.947		8	13		
G	Electrical field [kV]	1	15	504.9	-5.4117		14.48	-22.93		0.778	12.36	1	4	6		
		2	22.5	1,064.20	-4.4388		34.8	-27.67		1.09	11.378		10	15	2	
		3	30	1,013.50	2.3717	3	12.93	-21.27	3	0.706	9.79		6	12		**G3✓**
H	Cyclodextrin	1	0	795.1	-6.7250		22.89	-25.35		1.089	16.117	1	3	6		
		2	10 alpha	569	-4.0636		16.64	-22.02	2	0.6	9.725		6	9		
		3	20 beta	1,218.60	3.3098	3	22.79	-24.5		0.884	7.686		12	18	3	**H3✓**

Table 3.4: Tabulation of mean and S/N for four responses.
The four responses are area, migration time, symmetry and number of peaks for ‘Fingerprint’ Analysis.

3.1.3 Standard calibration and QC recovery

For both the ‘fingerprint’ and ‘all-in-one’ buffer systems, we obtained calibration curves as shown in Figure 3.4 and 3.5, respectively. A linearity range was obtained from 50 to 250 µmol/L at 95 % confidence limits. The QC recovery of 50 µmol/L (15 ppm) was within 100 ± 10%.

3.1.4 Wafer sample and spike recovery of 50 µmol/L DBS

The qualitative analysis of DBS on wafer surface was carried out with the ‘all-in-one’ buffer system. The wafer surface by manual swiveling method was found to contain no DBS in this concentration range. Nevertheless, if any of such DBS surfactant is presence on the wafer surface, it was suspected to be at ultra trace concentration level. Wafer surface was intentionally contaminated with 50 µmol/L of DBS (see Section 2.7). Spike recovery on wafer surface by manual swirling method was 100 ± 10%.

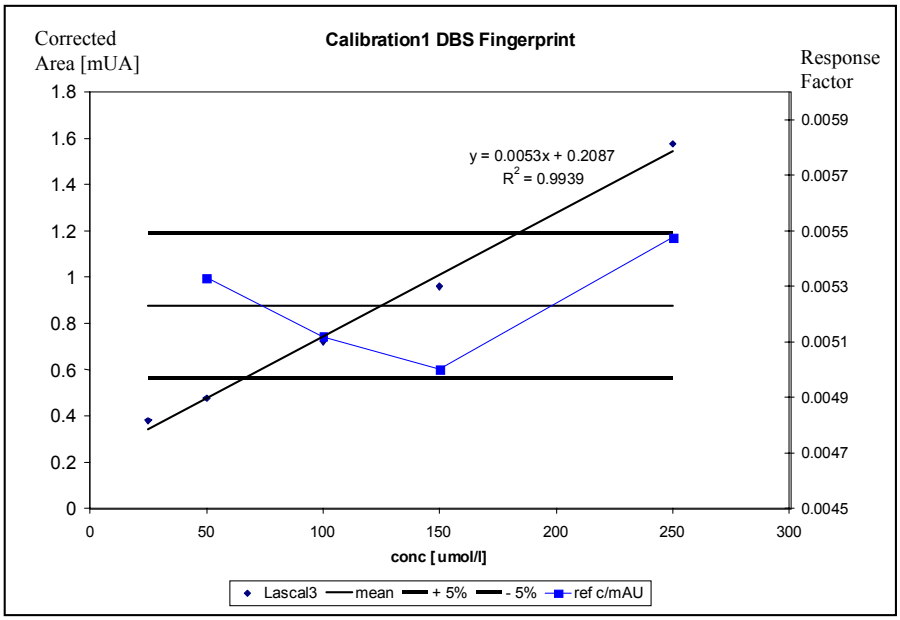

Figure 3.2: A calibration curve for DBS as 'fingerprint' buffer system.

Curve obtained from 25 µmol/L to 250 µmol/L. A linearity range 50 µmol/L to 250 µmol/L and 100 ±10% recovery of 50 µmol/L QC at 95% confidence limits.

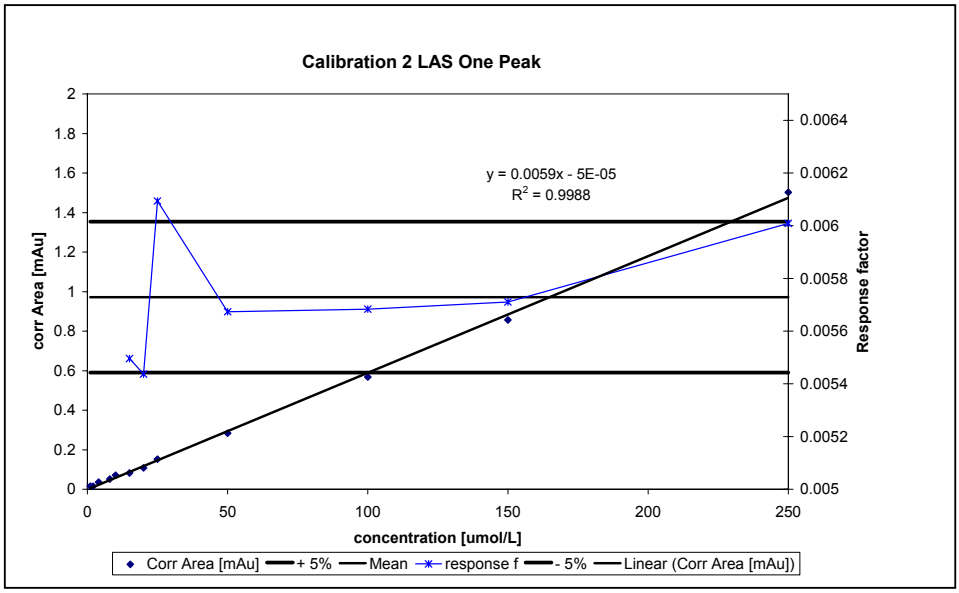

Figure 3.3: A calibration curve for DBS as 'all-in-one' buffer system.

Curve obtained from 25 µmol/L to 250 µmol/L. A linearity range 50 µmol/L to 250 µmol/L and 100 ±10% recovery of 50 µmol/L QC at 95% confidence limits.

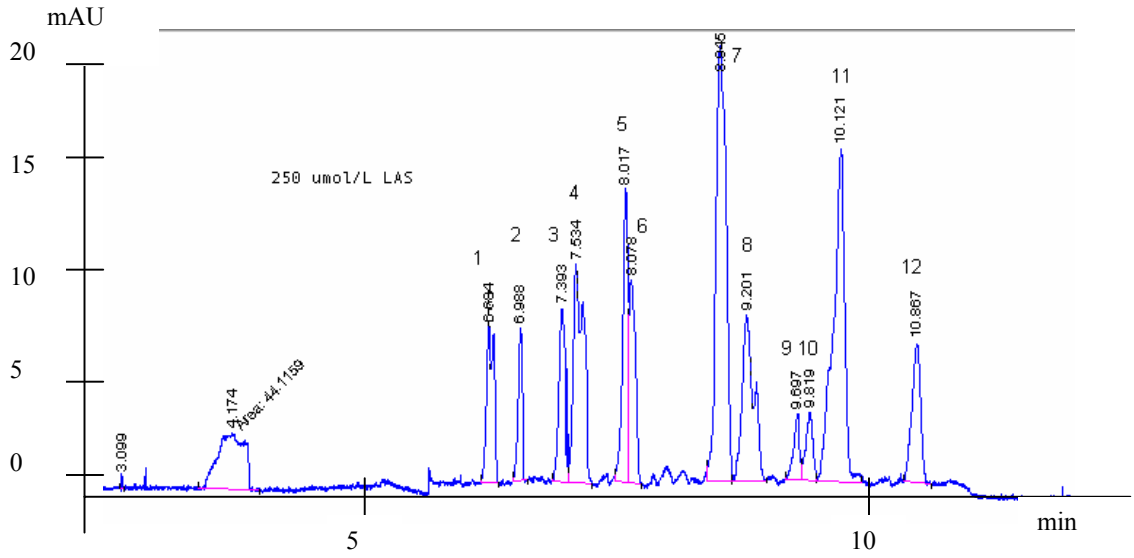

Figure 3.4: Electrophoregrams of a 'fingerprint' DBS analysis.

25mmol/L borate, pH 9, 50mmol/L SDS, 20-beta-CD, 50mbar@40s, 64.5cmx50µmD, -30kV, 20°C, 194/60. Sample was 250µmol/L dodecylbenzene sulfonate (DBS).

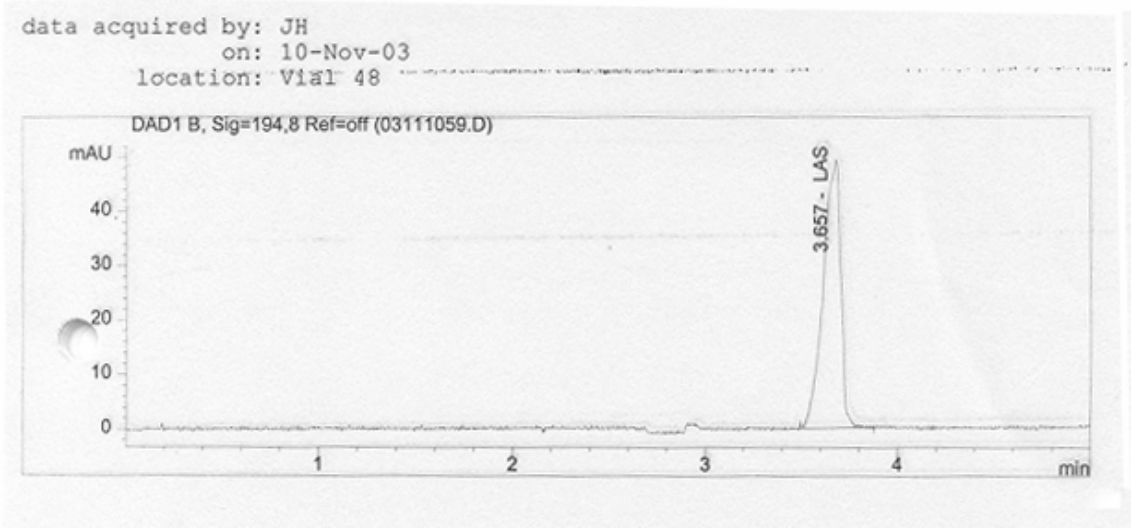

Figure 3.5: Electrophoregrams of a 'all-in-one' DBS analysis.

25mmol/L borate, pH 9, -30kV, 50 mbar@40s, 64.5 cm x 50 µm ID, 20°C, 194/60. Sample was 250µmol/L dodecylbenzene sulfonate (DBS).

3.2 Part II- Optimization of DBS analysis based on L_{16} Layout

3.2.1 Optimization of DBS buffer system by Taguchi

Based on a full randomization of the experimental order of L_{16} layout, the results were tabulated in an ANOVA table, Table 3.5A. The control factor E, buffer flushing, had the least source of variance. The change from a low level (2 minutes) to a high level (6 minutes) of flushing in the precondition step had the least importance to the overall performance. When factor E was selected as 'error', (e), new S' and ρ (rho) values were calculated, as shown in Table 3.5B. ρ values gave information about the influence of the factor. Factor G, B and D had ρ values <5%, showing that they can be neglected since they play no important role in the analysis. Hence, these parameters can be set to an easily adjusted parameter. These factors were pooled as shown in Table 3.5C. The main factors effecting the overall performance to achieve higher sensitivity at robust condition were factors F and C, injection mode and plug length of solvent before sample respectively. Similar results were illustrated graphically in terms of mean analysis and signal (S/N) analysis in Figure 3.6. The variance in the mean and the S/N graphs were less than 0.005 and 5 respectively for control factors of B, D, E and G. For factor A, S/N value was affected but not the mean value when a higher level of sample injection was adjusted. Control factors F and C were the most significant control factors since there were a larger variance of 0.02 mAU and 15 in the mean and S/N value respectively.

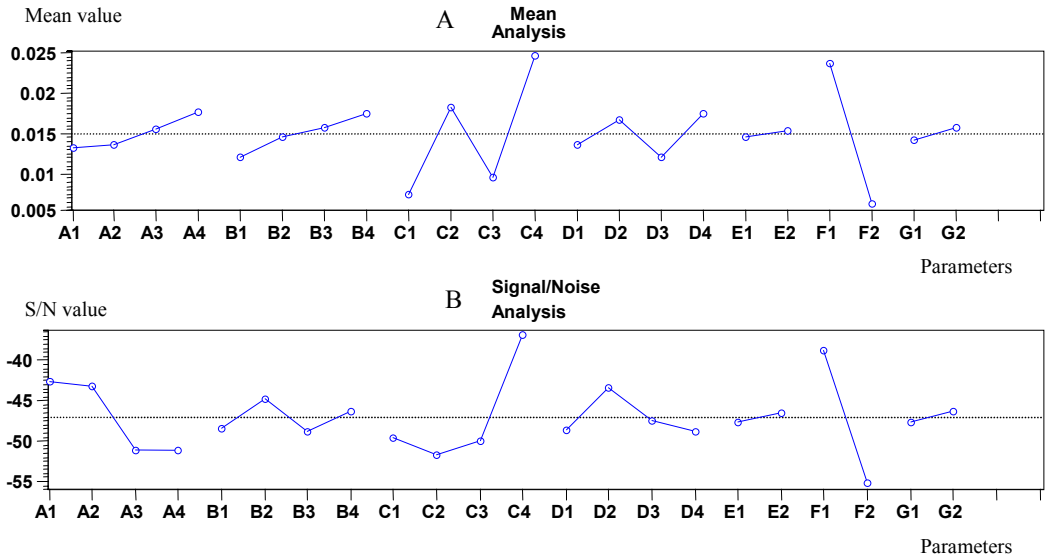

Figure 3.6: Result for the optimization experiment for DBS by ANOVA.

(A is Mean Value and B is Signal to Noise ratio. The response is Corrected Area ---- line represent the average mean and S/N values. A, B, C, D, E, F, G represent the seven parameters and 1, 2,3 represent the three levels (see Table 6)

Electrokinetic injection mode was intended to create a transient isotachophoretic pre-concentration to achieve a lower detection limit [18][37] for DBS. Theoretically, fluoride (F^-) ions would behave as the leading ions while the DBS ion as the terminating ions. However, the results in Table 3.5 and Figure 3.6 showed significant effect by hydrodynamic injection. Out of the 8 sets of experiments that are electrokinetically injected, it was suspected that this mode of injection was inter-dependent on the voltage ramp up rate and the sample size. A ramp rate slower than 0.5 min/kV and the injection time greater than 20 s did not show any peaks in the electrophoregrams for 30 min migration time analysis (Electrophoregrams not shown). Larger amount of anionic DBS at a lower voltage may take a longer time to migrate to the anode. On the other hand, hydrodynamic injection mode did not have problems with different injection times and ramp rates. Therefore, to obtain a robust buffer system, hydrodynamic was selected. Injection time at 10 s or 20 s had the highest S/N ratio. Moreover, large sample injected

may cause overloading. 20 s injection time was ideal to achieve 90% confidence limit. From Figure 3.6, factor D, voltage ramp rate, 0.5 min/kV shows only slightly higher S/N value than the other levels, thus there was not much effect which level to choose when hydrodynamic injection mode was selected. The other most significant factor shown in the ANOVA table and S/N graph was factor C, i.e. the amount of solvent/water plug. The different types of solvent or water were shown to have insignificant differences, but the solvent/water plug reduced the electric field from the sample zone to the buffer. The steeper the drop, the better the sample could be enriched. Acetone showed a slightly better S/N than the others, but it will be more practical to use water since acetone is volatile and more expensive. Water, like acetone, has no conductivity, and does not interact with the capillary wall. Furthermore, water has similar behavior to the buffer system. The effect of solvent/water plug on the overall performance was greatly significant only at length longer than 20 mm that is equivalent to 18.3 sec. The other factors related to the pre- and post-conditions of the capillary were less significant. In general, DBS is easily 'removed' by water or the buffer system and cross-contamination or memory effect is not present. Therefore, minimum flushing of the capillary with buffer between successive runs could be done. No post-conditioning of capillary after each run was required.

The Factor-Level chosen for the optimization of DBS at ultra trace level were as follows: A2, B1, C4, D2, E1, F1 and G1 (see Table 3.6), i.e.: Hydrodynamic injection for 20 s, 20 mm of water plug, 0.5 min/kV voltage ramp rate, 2 min of pre-flushing and without post flushing.

A: ANOVA before pooling of error.

Source	Pool	DF	S	V
A		3	270.0856	90.0285
B		3	44.42882	14.8096
C		3	570.0635	190.0211
D		3	71.90050	23.96683
E		1	4.855566	4.855566
F		1	1,072.341	1,072.341
G		1	7.524143	7.524143
(e)				
Total		15	2,041.199830	136.079989

B: ANOVA after factor E is selected as 'error', (e).

Source	Pool	DF	S	V	F	S'	ρ (rho)
A		3	270.0856	90.02854	18.54130	255.5189	12.5
B		3	44.42882	14.80960	3.050027	29.86212	1.46
C		3	570.0635	190.0211	39.13471	555.4968	27.2
D		3	71.90050	23.96683	4.935951	57.33380	2.81
E	(e)	1	4.855566	4.855566			
F		1	1,072.341	1,072.341	220.8479	1,067.486	52.3
G		1	7.524143	7.524143	1.549591	2.668577	0.13
(e)		1	4.855566	4.855566		72.83349	3.57
Total		15	2,041.199830	136.079989			

C: ANOVA after pooling of errors.

Source	Pool	DF	S	V	F	S'	ρ (rho)
A		3	270.0856	90.02854	5.595787	221.81976	10.87
B	(e)	3	44.42882	14.80960			
C		3	570.0635	190.0211	11.810899	521.79764	25.56
D	(e)	3	71.90050	23.96683			
E	(e)	1	4.855566	4.855566			
F		1	1,072.341	1,072.341	66.652142	1,056.2529	51.75
G	(e)	1	7.524143	7.524143			
(e)		8	128.7090	16.088629		241.329440	11.82
Total		15	2,041.199	136.079989			

Source - factor name or error (e)
Pool - column with buttons to pool/unpool source contribution
DF - source degree of freedom, f
S - source variation
V - source variance, V=S / f
F - source variance ratio, F = V / Ve , where Ve is pooled variance
S' - source pure variation, S' = S - Ve . f
ρ (rho) - source contribution ratio (percentage) ρ = S' / St 100%, where St is total variation
(e) - represents pooled sources of primary error which caused by the error of experimental condition setting, etc. is different from experiment to experiment and secondary error which caused by the error or difference(s) between samples or between measurements

Table 3.5: Results of ANOVA on optimization of Ultra trace analysis of DBS.
A-Injection Time; B-type of solvent before sample; C-plug length before sample; D-voltage ramp; E-buffer flushing; F-mode of injection; G-water flush post condition

	Factor Name	Choice Level
A	Injection Time [sec]	20
B	type of solvent before sample	water
C	plug length before sample [mm]	20
D	voltage ramp [min]	0.5
E	buffer flushing [min]	2
F	mode of injection	hydrodynamic
G	water flush post condition [sec]	0

Table 3.6: Choice of Parameters for ultra trace analysis of DBS.
All peaks were detected by direct photometeric detection at 200 nm at a constant temperature of 20°C. Fused silica capillaries, 50μmm ID, a total length of 64.5cm (56 cm to the detection window).

3.2.2 Confirmation run for L_{16} experiment

A 'confirmation' analysis was carried out to make sure the choices for the optimized system was as predicted. 5 μmol/L DBS was injected hydrodynamically for 20 sec before the 20-mm water plug had a mean corrected area 0.80 mAU at 4 sec and standard deviation of 0.002 (n=18) (see Figure 3.11).

3.2.3 Standard calibration, QC recovery, LOQ and LOD determination

An average calibration curve was obtained based on 10 different runs of calibration standards. The range of 0.025 to 100 μmol/L had two linearity curves; one range from 10 to 100 μmol/L, and the other 0.20 to 5 μmol/L, (Figure 3.7, 3.8 respectively). Another set

of calibration standards where a 10 µmol/L of hydrofluoric acid (HF) was added as a matrix matching real samples containing HF were carried out. The linearity was same as the one without HF matrix (Figure 3.9). The quality check (QC) recovery of another set of standards of DBS was within 100 ± 10% for concentrations of 2.5 µmol/L and 5 µmol/L (Table 3.7). The percent recovery was lower for samples containing HF, maybe due to higher noise. However, it was still acceptable. Figure 3.10 showed the absence of any cross-contamination since the baseline was straight and smooth. According to DIN 32645 calibration method, Figure 3.8 and 3.9, the limit of detection (LOD) is 0.2 µmol/L and 0.22 µmol/L and the limit of quantification (LOQ) is 0.75 µmol/L and 0.82 µmol/L at 95% confidence level. The system has a good standard deviation (SD) and method's coefficient of variation of 0.10 and 11% respectively. With the used of a high-resolution detection cell, the sensitivity increased by 10 fold. 5 µmol/L standard DBS was measured using 2 different detector cells, Figure 3.11 and 3.12 respectively. By comparing these two electrophoregrams, the area under the peak, mAU, showed an increase from 0.8 to 8, a 10-fold improvement from a normal cell to a high-resolution detector cells respectively. Therefore, the LOD and LOQ will be improved to 0.02 µmol/L and 0.08 µmol/L, i.e. 6.5 ppb and 24.5 ppb respectively. With this low level of detection, ultra trace level of surfactant as DBS on wafer surface will be detectable and quantifiable.

QC recovery				
	without HF		with HF	
	2.5 µmol/L	5.0 µmol/L	2.5 µmol/L	5.0 µmol/L
Data [µmol/L L]	2.384	5.392	2.198	4.000
QC Recovery [%]	95.34	107.84	87.92	80.00
SD	0.225	0.367	0.083	0.147

Table 3.7: Results on QC Recovery for ultra trace DBS analysis.

Corrected Area [mUA]

Response Factor

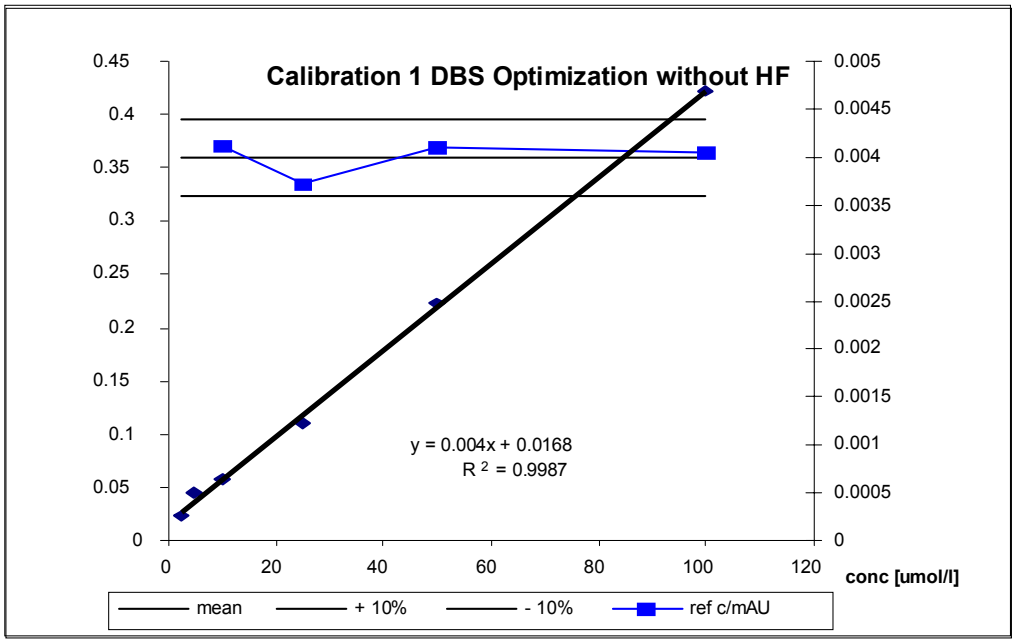

Figure 3.7: A calibration curve for DBS analysis at higher concentration range.

Curve from 0.25 µmol/L to 100 µmol/L without hydrofluoric acid (HF) matrix. A linearity range is 10 µmol/L to 100 µmol/L 90% confidence limits.

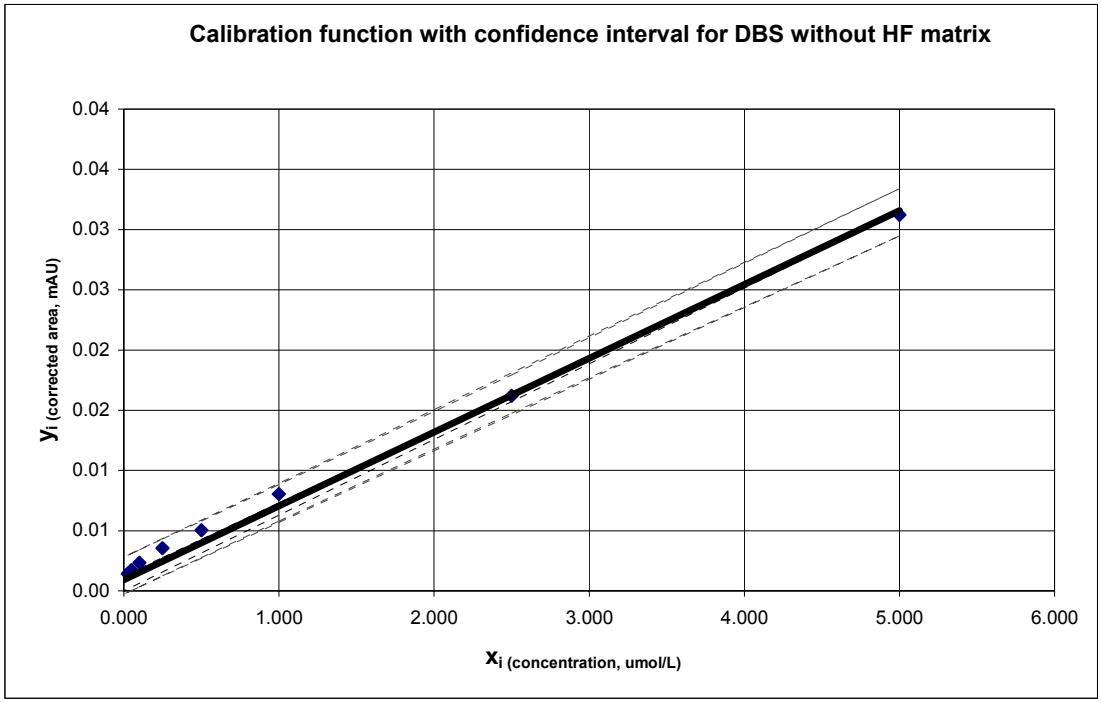

Critical value, Limit of Detection, Limit of Decision and Limit of Quantification :

(DIN 32 645; with t(95%;f) single-sided for y_c, x_{LOD}, x_{LODec} and t(95%;f) double-sided for x_{LOQ})

y_c	**0.00**	x_{LODec}	**0.41**
x_{LOD}	**0.20**	x_{LOQ}	**0.75**

Method data :

N =	8		
Slope a_1 =	**0.006**	CI(a_1)	**0.0003**
intercept a_0 =	**0.001**	CI(a_0)	**0.0015**
Standard deviation s_{y1}		**0.001**	
Standard deviation of the method s_{x0}			**0.097**
Method's coefficient of variation V_{x0}			**10.3%**

Linearity test

calibration function is

linear	**X**
not linear	

Correlation:

R= 0.9995

Figure 3.8: A calibration curve for DBS analysis at lower concentration range.

Curve from 0.025 µmol/L to 5 µmol/L without hydrofluoric acid (HF) matrix. A linearity range is 0.20 µmol/L to 5 µmol/L 95% confidence limits.

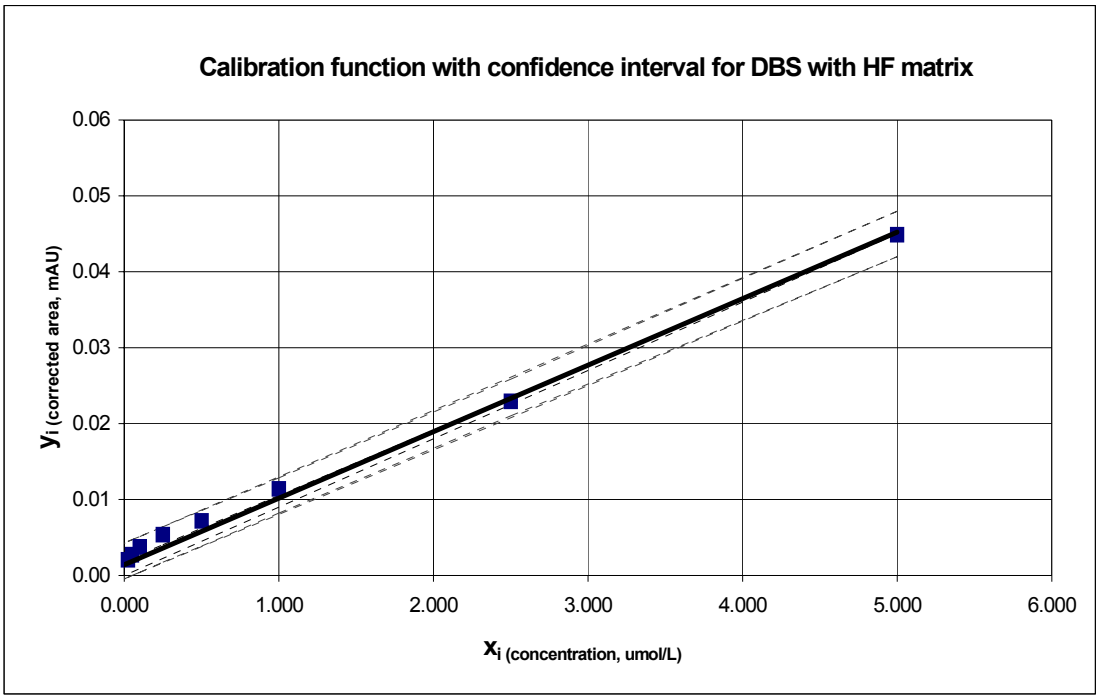

Critical value, Limit of Detection, Limit of Decision and Limit of Quantification :			
(DIN 32 645; with t(95%;f) single-sided for y_c, x_{LOD}, x_{LODec} and t(95%;f) double-sided for x_{LOQ})			
y_c	**0.00**	x_{LODec}	**0.43**
x_{LOD}	**0.22**	x_{LOQ}	**0.81**

Method data :					Linearity test	
Slope a_1 =	**0.009**	CI(a_1)	**0.0005**		calibration function is	
intercept a_0 =	**0.002**	CI(a_0)	**0.0024**		linear	**X**
					not linear	
Standard deviation s_{y1}		**0.001**				
					Correlation:	
Standard deviation of the method s_{x0}			**0.104**			
Method's coefficient of variation V_{x0}			**11.0%**		R= 0.9993	

Figure 3.9: A calibration curve for ultra trace DBS analysis with HF matrix.

Curve from 0.025 µmol/L to 5 µmol/L with hydrofluoric acid (HF) matrix. A linearity range is 0.20 µmol/L to 5 µmol/L 95% confidence limits

3.2.4 Wafer sample analysis and spike recovery

The analysis results for VPD-WSPS scanning; VPD-manual swirling and non-VPD-manual swirling method did not show the presence of surfactant as DBS on 200-mm wafer surface (Figure 3.10). 80 wafers were analysed on different days and the results are tabulated in Tables 3.8-3.12. A known amount of standard DBS was added into the vial containing the wafer sample solution. The recoveries of the spike sample were within 100 ± 10% with standard deviation (SD) of 0.2 – 0.6 (n=30) as shown in Table 3.8, 3.9. This showed that this optimized buffer system for DBS analysis was reproducible. The recovery for VPD-WSPS method was slightly lower, and the SD was higher. This may be due to complicated high concentration Si-matrix in the 100 μL extracted sample volume. The recovery of contaminated wafer for VPD-WSPS was too low to be acceptable. Theoretically, VPD-WSPS scanning method is superior to swirling method with the following advantages: 1) Lower concentration can be detected with small volume of extraction solution; 2) no cross-contamination caused by human error; 3) does not require skilled worker to prepare the wafer sample. However, data showed that VPD-WSPS extraction method for DBS was the worst.

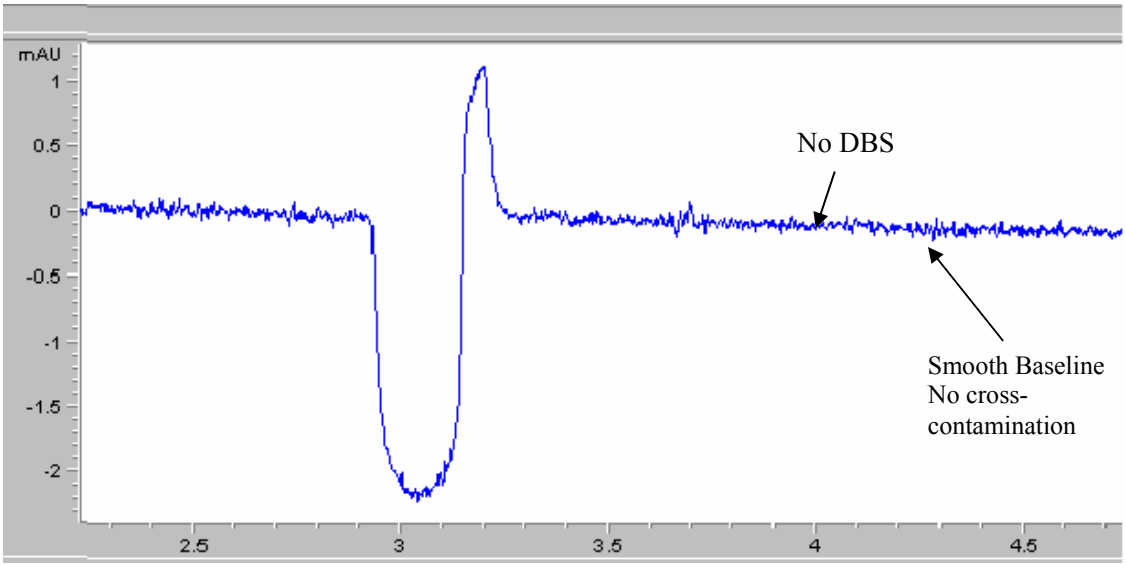

Figure 3.10: Electrophoregram of wafer sample by manual swiveling method.

Absence of DBS peak in from wafer surface all three methods of extraction.

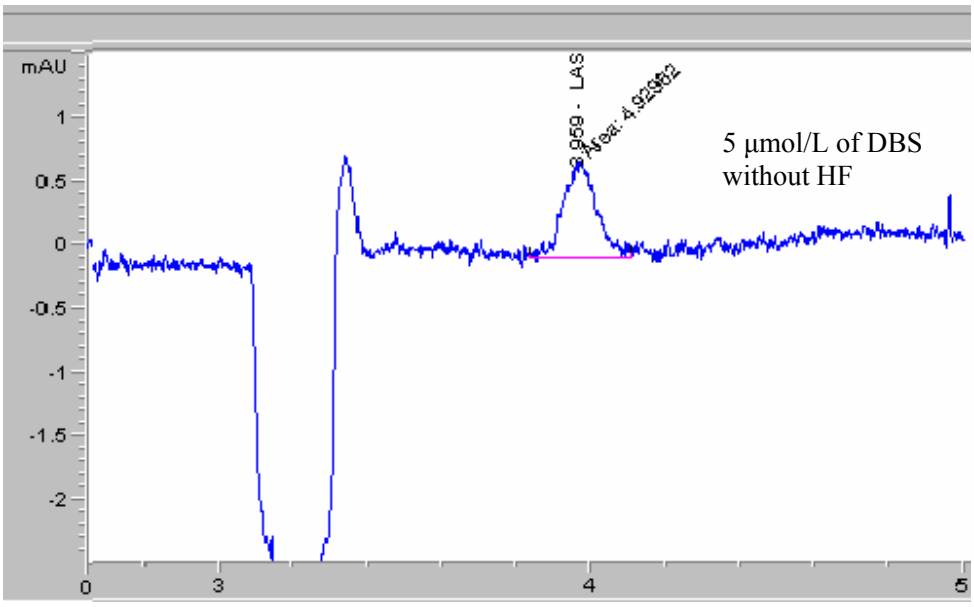

Figure 3.11: Electrophoregram of 5 µmol/L DBS vial spike.

% Recovery for manual swiveling and VPD-manual extraction method is 100%±5%.

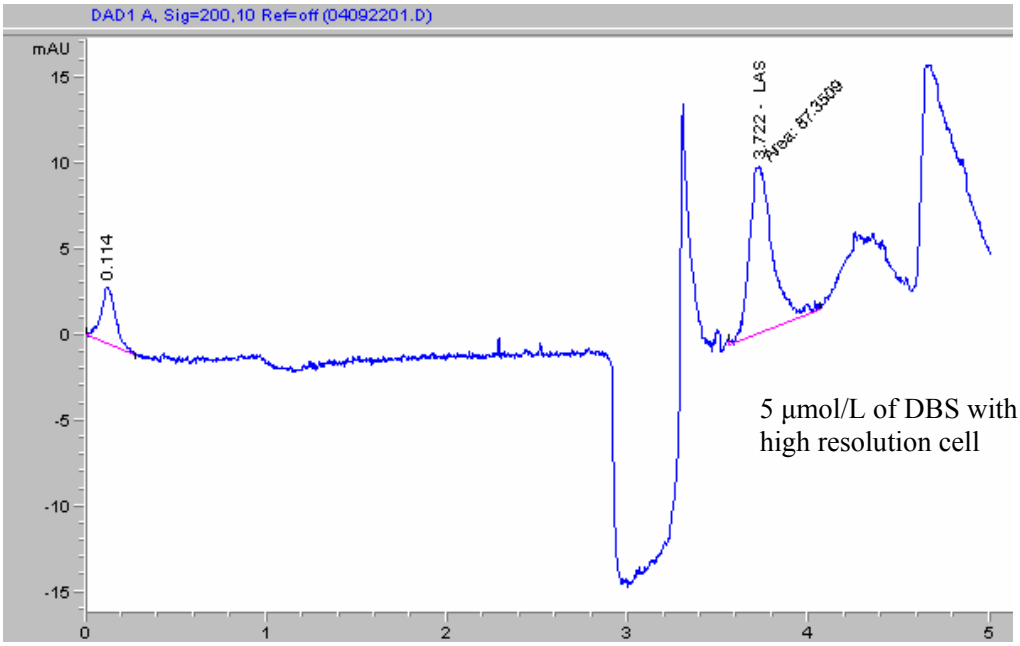

Figure 3.12: Electrophoregram of 5 µmol/L DBS by high-resolution detector cell.

Therefore, further test was carried out to determine the root cause of the poor extraction recovery. Firstly, the extraction time was lengthened from 5 min (2 ways round the wafers) to 10 min (4 ways round the wafers). Secondly, saturation of extraction solution was ensured. In Table 3.10, the increase of extraction time showed a slight improvement in the recovery of 30 %. By increasing the spike concentration from 10 µmol/L to 20 µmol/L, a reduction of recovery was obtained. Table 3.11 showed a similar increase of % recovery when extraction time was increased. However, when the scanned wafers were re-scanned, some DBS still can be detected. This proved that incomplete extraction occurred, even when the contaminated wafers were scanned for 10 min. In Table 3.12, increasing the extraction samples volume from 100 µL to 200 µL for the extraction of 5 µmol/L and higher did not show much difference. Nevertheless, a lower concentration of contamination spike, 0.5 µmol/L had a higher % recovery. This showed that over-

saturation occurred for the extraction of more than 0.5 µmol/L with 200 µL by VPD-WSPS method.

Finally, an in-house surfactant was measured for confirmation of the optimized DBS system. Although there were several noise peaks, the DBS peak was clearly shown at 4.1 sec (Figure 3.13). The system was robust enough to measure the complicated matrix in-house surfactant at a 1000 times diluted concentration of 4.679 µmol/L, Table 3.13. The actual concentration of DBS in this surfactant was 4679 µmol/L (1522 ppm).

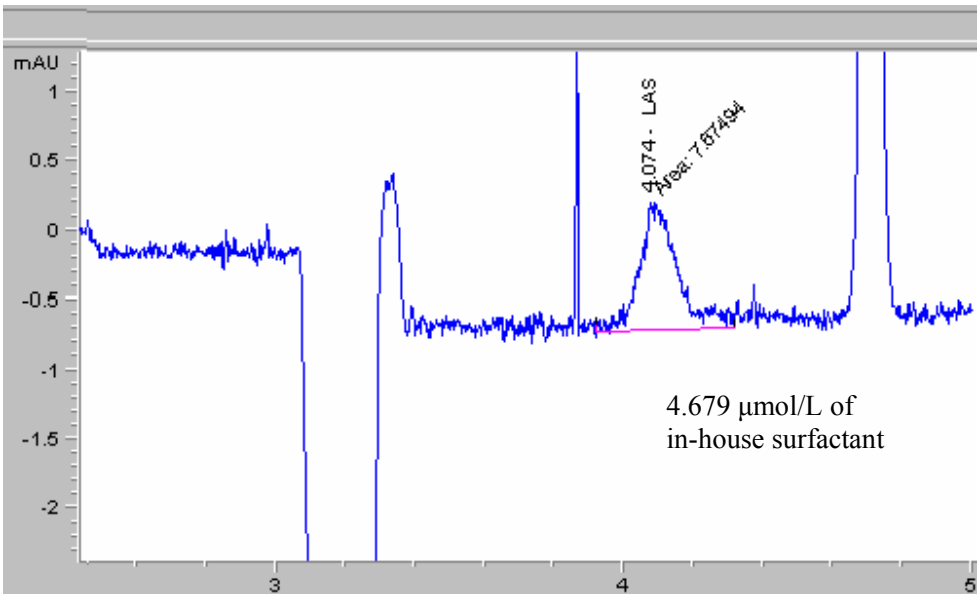

Figure 3.13: Electrophoregram of an in-house surfactant.

Average 2 wafers; 4 replicates (- means not measured.)			
	Manual Swirling 5.0 µmol/L Spike	VPD-manual 5.0 µmol/L Spike	VPD-WSPS 10 µmol/L Spike
Wafer Sample [µmo/L]	0.000	0.000	0.000
Vial Spike [µmo/L]	5.273	-	5.410
Vial Spike Recovery (%)	**105.47**	**-**	**108.21**
SD	0.272	-	0.686
Wafer Spike [µmo/L]	5.157	4.834	4.406
Wafer Spike Recovery (%)	**103.14**	**96.67**	**44.06**
SD	0.493	0.571	0.936
Vial & Wafer Spike [µmo/L]	10.327	9.354	8.382
Vial & Wafer Spike Recovery (%)	**103.27**	**93.54**	**55.88**
SD	0.591	0.536	1.469

Table 3.8: Day 1 analysis of wafer and % Recovery.

Average 1 wafer; 10 replicates; 10 data			
	Manual Swirling	VPD-manual	VPD-WSPS
Wafer Sample [µmol/L]	0.000	0.000	0.000
Vial Spike [µmol/L]	5.126	5.199	5.187
Vial Spike Recovery (%)	**102.53**	**103.99**	**103.74**
SD	0.315	0.340	0.441
Wafer Spike [µmol/L]	5.002	5.073	0.812
Wafer Spike Recovery (%)	**100.04**	**101.46**	**16.25**
SD	0.396	0.330	0.849
Vial & Wafer Spike [µmol/L]		9.794	
Vial & Wafer Spike Recovery (%)		97.94	
SD		0.41	
Average 3 wafers; 10 replicates each; 30 data			
	Manual Swirling	VPD-manual	VPD-WSPS
Vial Spike [µmol/L]	5.110	5.110	4.056
Vial Spike Recovery (%)	**102.21**	**102.21**	**81.13**
RSD	0.45	0.33	1.44
Wafer Spike [µmo/L]	5.034	5.086	1.244
Wafer Spike Recovery (%)	**100.67**	**101.73**	**24.89**
SD	0.41	0.31	1.20
Vial & Wafer Spike [µmo/L]		9.813	
Vial & Wafer Spike Recovery (%)			
SD		0.481	

Table 3.9: Day 2 analysis of wafer and % Recovery.

WSPS Extraction, 3 wafers; 9 replicates			
Wafer Spike	Spike 10umol/L 2 Ways Scanning	Spike 20umol/L 2 Ways Scanning	Spike 10umol/L 4 Ways Scanning
Wafer [µmo/L]	0.000	0.000	0.000
Spike [µmo/L]	0.9682	0.7137	3.0870
Wafer Spike Recovery [%]	9.68	7.14	30.87
SD	0.94	0.96	4.74

Table 3.10: Measurement of DBS at different concentrations and scanning by WSPS.

WSPS Extraction, 5 replicates						
Wafer Spike	#1 Spike 10umol/L 2 Ways Scanning	Rescan #1 Spike 10umol/L 2 Ways Scanning	#2 Spike 10umol/L 2 Ways Scanning	Rescan #2 Spike 10umol/L 2 Ways Scanning	#3 Spike 10umol/L 4 Ways Scanning	Rescan #3 Spike 10umol/L 4 Ways Scanning
Wafer [µmo/L]	0.000		0.000		0.000	
Spike [µmo/L]]	**0.031**	**1.569**	**1.763**	**0.595**	**1.873**	**1.090**
Wafer Spike Recovery [%]	0.31	15.69	17.63	5.95	18.73	10.90
SD	**0.05**	**0.47**	**0.59**	**0.53**	**0.37**	**0.49**

Table 3.11: Re-measurement of DBS by re-scanning with WSPS.

WSPS, 200uL water for scanning; 2 replicates					
Wafer Spike	0.5umol/L 2 Ways Scanning, 100 uL	0.5umol/L 2 Ways Scanning, 200 uL	5.0umol/L 2 Ways Scanning, 200uL	10umol/L 2 Ways Scanning, 200 uL	10umol/L 4 Ways Scanning, 200uL
Wafer [µmo/L]	0.000	0.000	0.000	0.000	0.000
Spike [µmo/L]	0.311	0.079	5.319	0.935	1.142
Wafer Spike Recovery [%]	62.22	15.88	53.19	9.35	11.42
SD	0.440	0.066	4.006	0.645	0.477
Wafer Spike			Rescan 5umol/L 2 Ways Scanning, 200ul	Rescan 10umol/L 2 Ways Scanning, 200 uL	Rescan 10umol/L 4 Ways Scanning, 200 uL
Wafer [µmo/L]			0.000	0.000	0.000
Spike [µmo/L]			1.789	1.480	1.120
Wafer Spike Recovery [%]			17.89	14.80	11.20
SD			2.526	0.522	0.188

Table 3.12: Measurement of DBS with larger extraction volume.

In-house surfactant Spike recovery 10 replicates			
	Sample 1000X dil	Sample 1000X dil + 5spike	**Actual Sample Conc**
Data [µmo/L]	4.679	8.813	**4678.8** µmo/L
Recovery [%]	-	82.68	**1522 ppm**
SD	0.192	0.618	

Table 3.13: Measurement of In-house surfactant sample.

4. Conclusion

In Part I, based on the Taguchi data plots, the 'fingerprint' analysis showed that the four responses had similar results for all of the factors except for the concentration of SDS. Theoretically, SDS helps to improve the separation. Therefore, this factor is 'trade-off' to the level that has the highest number of peaks. The best combination for the factor-level for this system is A2, B1, C3, D1, E1, F2, G3 and H3. Hence, the 'fingerprint' system is 25 mmol/L borate electrolyte buffer system with 25 mmol/L of SDS and 20 μmol/L of β CD modifiers, at pH 9 and 30 kV. As for the 'all-in-one' analysis, there is no conflict in all of the responses. Thus, the best combination for the factor-level is A2, B1, C3, D1, E1, F1, G3 and H1. Hence, the 'all-in-one' system is 25 mmol/L borate electrolyte buffer system at pH 9 and 30 kV, without any modifiers. The confirmation experiments for both buffer systems have positive and consistent results. The linearity range is from 50 to 250 μmol/L at 95 % confidence limits. And the QC recovery is 100 ±10%. The analysis of the real sample, 200-mm wafer surface in the presence of high hydrofluoric acid matrix, the result is below the detection limit. However, this method is validated when a spike DBS has a good recovery of 100 ± 10%.

In Part II, a lower detection limit for trace analysis of DBS is achieved. The 'all-in-one' buffer system is further optimized to sub-ppb level with the Taguchi $\boldsymbol{L_{16}}$ design matrix. The ANOVA table showed that the main effects are the mode of injection and the preconcentration sample plug where the ρ values are greater than 5 %. The data plot for both the mean plot and the S/N plots show the similar results, where the hydrodynamic injection is much preferred than electrokinetic injection and the larger the solvent plug

gives higher sensitivity. With the confirmation experiment, this optimized buffer system is able to get a significant single DBS peak in the presence of high HF matrix. The linearity range extends from 0.5 to 5 μmol/L and the QC recovery is between 80% and 108% in vapor phase decomposition (VPD)-matrix. The wafer surface analysis is still not detected, but the spike recovery on the surface is 100 ±10%. The in-house surfactant is analysed to have a concentration of 1522 ppm of DBS.

Taguchi methodology is shown a powerful and systematic tool. It is successfully applied in the determination of main parameters effecting the DBS analysis at a short and non-complicated design of experiment. For $\boldsymbol{L_{18}}$ design matrix, only 18 experiments are carried out, only by switching the S/N equation, the sensitivity and the qualitative analysis can be evaluated simultaneously. It is not necessary to run another set of experiment to determine different responses. Furthermore, Taguchi incorporate the 'noise' factor into the test matrix, which allows the experimental data to be more robust.

With the application of high-resolution detector cell in the optimized method, the detection limit of DBS analysis is improved by 10-fold at sub-ppb level. The limit of detection (LOD) and limit of quantification (LOQ) are calculated to be 6.5 ppb and 24.5 ppb respectively.

In conclusion, the results obtained in this report provide a robust method for analysis anionic surfactant, dodecylbenzene sulfonates, DBS by CE at 6.5 ppb detection limit.

5. Future Work

In the fast growing semiconductor technology, small design route on wafer chip manufacturing is evolving in near further. The cleanliness and purity of wafer surface are becoming more critical as prerequisites for many wafer manufactures. Therefore, a low detection limit for the analysis of ionic surfactant will be required at parts per trillion (ppt) trace levels. Therefore, the evaluation of test method for other anionic and cationic surfactant beside DBS will be worth for further investigation. A routine test method for the determination of both anionic and cationic surfactant in a single analysis is ideal for shorter throughput in a fast moving industry.

Detection limits of anionic surfactants by capillary electrophoresis can be further reduced by considering the optimum capillary temperature, the length and diameter of the column, mixture of solvents, addition of divalent cations, injection technique by sweeping or both stacking and sweeping, etc. The used of conductivity detector may enhance the sensitivity for the detection of ions by CE.

The development of higher sensitivity method of extracting surfactant from the wafer surface is also critical. The reduction of extraction sample solution may improves the method of detection, however, the minute sample size may contain high HF from the VPD extraction method, which will resultant in large ‘noise’ peak during data quantification.

6. References

[1] http://lookwayup.com

[2] M.R. Porter, *Recent Developments in the Analysis of Surfactants*, SCI by Elsevier Applied Science, London and New York, 1991, p137-157, 188-215.

[3] T. Hattori and K.Saga, *Ultraclean Surface Processing of Silicon Wafers-Secrets of VLSI Processing*, Springer-Verlag, New York, 1998, pp. 39-41, 123-130.

[4] J. Cross, Anion Surfactants –An Introduction, New York : Marcel Dekker, c1998, pp. 2-31.

[5] J. R. Bodenmiller and H.W. Latz. Determination of Alkylbenzenzesulfonate and Alkylsufate Homologs, after Electrophoretic Separation Using Aqueous Dioxane Agarose Gels. *Anal. Chem.* **44**: 926-930 (1972)

[6] McAvoy, J. And W. Giger. Determination of linear alkylbenzene sulfonates in sewage sludge by high resolution gas chromatography/mass spectometry. *Environ. Sci. Technol.* **20:** 376-383 (1986).

[7] H. Hon-Nami and T. Hanya. Gas-Liquid Chromatographic-mass Spectrometric. Determination of Alkylbenzenesulfonates in River Water. *J. Chromatography,* **161**: 205-212 (1978).

[8] K.Heinig, C.Vogt and G. Werner. Separation of ionic and neutral surfactants by Capillary electrophoresis and high-performance liquid chromatography. *J. Chromatography A.* **745**: 281-292 (1996).

[9] M. Kaikhtman, J. S. Rohrer. Determinations of fluorochemical surfactants in acid etch baths by ion chromatography with on-line matrix elimination. *J. Chromatography A.* **822**: 321-325 (1998).

[10] P.L. Desbène, C.Rony, B. Desmazières and J.C. Jacquier. Analysis of alkyaromatic sulphonates by high-performance capillary electrophoresis. *J. Chromatography A.* **608**: 375-383 (1992).

[11] P.L. Desbène and C.Rony, Determination by high-performance capillary electrophoresis of alkyaromatics used as bases of sulfonation in the preparation of industrial surfactants. *J. Chromatography A.* **689**: 107-121 (1995).

[12] H. Salimi-Moosavi and R.M. Cassidy. Application of Nonaqueous Capillary Electrophoresis to the Separation of Long-Chain Surfactants. *Anal. Chem.* **68**: 293-299 (1996).

[13] W.H Ding and C.H. Liu. Analysis of Linear alkylbenenzesulfonates by capillary zone electrophoresis with large-volume sample stacking. *J. Chromatography A*. **929**: 143-150 (2001).

[14] K. Heinig, C.Vogt. and G. Werner. Determination of linear alkylbenezensulfonates in industrial and environment samples by capillary electrophoresis. *Analys*t. **123**: 349-353 (1998).

[15] R. Loos and R. Niessner. Analysis of aromatic sulfonates in water by solid-phase extraction and capillary electrophoresis. *J. Chromatography A*. **822**: 91-303 (1998).

[16] Th. Ehmann, L.Fabry, J.Moreland and J. Hage. Ion Chromatography and Capillary Electrophoresis in Large-Scale Manufacturing of Semiconductor Silicon. *Semiconductor FabTech 12th Ed.* pp. 71-77.

[17] Th. Ehmann, L. Fabry, H. Rufer, L. Kotz, S. Pahlke, C. Mantler. Modification and validation of the pyromellitic acid electrolyte for the capillary electrophoretic determination of anions. *J. Chromatography A.* **995**: 217-226 (2003).

[18] Th. Ehmann, L. Fabry, L. Kotz, S. Pahlke. Ultra-trace analytical monitoring of silicon wafer surfaces by capillary electrophoresis. *Freseiu J. Anal. Chem.* **371**: 407-412 (2001).

[19] Th. Ehmann, K. Bächmann, L. Fabry, H. Rüfer, M. Serwe, G. Ross, S. Pahlke, L. Kotz. Capillary preconditioning for analysis of anions indirect UV detection in capillary zone electrophoresis Systematic investigation of alkaline and acid prerinsing techniques by designed experiments. *J. Chromatography A.***816**: 261-275 (1998).

[20] S.F.Y. Li. Capillary Electrophoresis Principles, Practice and Applications., Vol 52. Elsevier Science, The Netherlands 1992, pp. 1-30; 201-226.

[21] P.D. Grossman and J.C.Colburn. Capillary Electrophoresis Theory and Practise. San Diego : Academic Press , c1992, pp. 301-341.

[22] V.Johan and P. Sandra. Introduction to micellar electrokinetic chromatography. Heidelbery, 1992, pp.3-11,55-67,111-129.

[23] G. Norberto A. Capillary Electrophoresis Technology, Chromatographic Science ; Vol 64. New York Marcel Dekker, Inc., 1993.

[24] D. N. Heiger. High Performance Capillary Electrophoresis –An Introduction. Hewlett-Packard, 1992, pp5-74.

[25] F. Haddadian, D.A. Shamsi and I.M. Warner. Separation of Saturated and Unsaturated Free Fatty Acids Using Capillary Electrophoresis with Indirect Photometric Detection. *J. Chromatographic Science.* **37**: 103-107(1999).

[26] P.L. Zhu, D.H. Marchand and J.W. Dolan. Para-Hydroxybenzoic Acid as an Indirect Detection Buffer in Capillary Zone Electrophoresis. *Chromatographia.* **50**: 321-324 (1999).

[27] J.L. Beckers. UV detection in capillary zone electrophoresis Peaks or dips – that is the question. *J. Chromatography A.* **679**: 153-165 (1994).

[28] F.Foret, S.Fanali, L.Ossicini and P.Boek. Indirect Photometeric Detection in Capillary Zone Electrophoresis. *J. Chromatography* **470**: 299-308 (1989).

[29] M. A Friedberg, M. Hinsdale, Z.K. Shihabi. Effect of pH and ions in the sample on stacking in capillary electrophoresis. *J. Chromatography A*. **781**: 35-42 (1997).

[30] M.P. Harrold, M.J. Wojtusik, J. Rivielo and P. Henson. Parameters influencing separation and detection of anions by Capillary electrophoresis. *J. Chromatography*. **640**: 463-471 (1993).

[31] K. D. Altria, B. J. Clark, M. A. Kelly. Investigation into the effects of Sample Dissolving Solvents and Smaple Matrices on the Separation Obtained in Capillary Electrophoresis. Part II. MECC. *J. High Resol. Chromatogr*. **22**: 55-58 (1999).

[32] K.D. Altria and S.M. Bryant. Highly Selective and Efficient Separations of a Wide Range of Acidic Species in Capillary Electrophoresis Employing Non-Aqueous Media. *Chromatographia*. **46**: 122-130 (1997).

[33] M.J. Cugat, F. Borrull and M. Calull. Comparative study of capillary zone electrophoresis and micellar electrokinetic capillary chromatography for the separation of naphthalenedisulfonate isomers. *Analyst*. **125**: 2236-2240 (2002).

[34] Th. Ehmann, K. Bächmann, L. Fabry, H. Rüfer, S. Pahlke and L. Kotz. Optimization of the Electrokinetic Sample Introduction in Capillary Electrophoresis for the Ultra Trace Determination of Anions on Silicon wafers Surfaces. *Chromatographia.* **45**: 301-311 (1997).

[35] W.R. Jones and P. Jandik. Various approaches to analysis of difficult sample matrices of anions using capillary ion electrophoresis. *J. Chromatography.* **608**: 385-393 (1992).

[36] T. Soga. Analysis of Inorganic and Organic Anions by Capillary Zone Electrophoresis. Application Note. Hewlett Packard.

[37] S. Chen and D. J. Pietrzyk. Separation of Sulfonate Surfactants by Capillary ElectrohphoreisL Effect of Buffer Cation. *Anal. Chem.* **65**: 2770-2775 (1993).

[38] Y.He and H.K. Lee. Large-Volumne Sample Stacking in Acidic Buffer for Analysis of Small Organic and Inorganic Anions by Capillary Electrophoresis. *Anal. Chem.* **71**: 995-1001 (1999).

[39] D. Martínez, F. Borrull and M. Calull. Sample Stacking using field-amplified sample injection in capillary zone electrophoresis in the analysis of phenolic compounds. *J. Chromatography A.* **788**: 185-193 (1997).

[40] D. S. Burgi and R.L. Chen. Optimization of Sample Stacking for High-Performance Capillary Electrophoresis. *Anal. Chem.* **63**: 2042-2047 (1991).

[41] M. J. Woktusik and M. P. Harrold. Factors influencing trace ion analysis with preconcentration by electrostacking. *J. Chromatography A.* **671**: 411-417 (1994).

[42] R.Stevenson, R. Weinberger and U. D. Neue. Separation Solutions Capillary Electrophoresis with Sweeping Stacking. American Laboratory. December (2001).

[43] J. P Quirino, J. B. Kim, S. Terabe. Sweeping: concentration mechanism and application to high-sensitivity analysis in capillary electrophoresis. *J. Chromatography A.* **965**: 357-373 (2002).

[44] J. P Quirino, S. Terabe, P. Bocek. Sweeping of Neutral Analytes in Electrokinetic Chromatography with High-Salt-Containing Matrixes. *Anal. Chem.* **72**: 1934-1940 (2000).

[45] L. Zhu, C.Tu and H.K. Lee. On-line Concentration of Acidic Compounds by Anion-Selective Exhaustive Injection-Sweeping-Micellar Electrokinetic Chromatography. *Anal. Chem.* **74**: 5820-5825 (2002).

[46] W. Shi and C. P. Palmer. On-column sample preconcentration in electrokinetic chromatography by sweeping with polymeric pseudo-stationary phases. *J. Sep. Sci.* **25**: 215-221 (2002).

[47] J. P Quirino and S. Terabe. Sweeping with an Enhanced Electric Field of Neutral Analyte Zone in Electrokinetic Chromatography. *J. High Resol.* **22**: 1367-372 (1999).

[48] J. P Quirino and S. Terabe. Sweeping of Analyte Zone in Electrokinetic Chromatography. *Anal. Chem.* **71**: 1638-1644 (1999).

[49] H. Siren, R. Sulkava. Determination of black dyes from cotton and wool fibres by capillary zone electrophoresis with UV detection: application of marker technique. *J. Chromatography A.* **717**: 149-155 (1995).

[50] M. A. Janusa, L. J. Andermann, N. M. Kliebert and M. H. Nannie. Determination of Chlorate Concentration Using Capillary Zone Electrophoresis. *J. Chem. Edu.* **75**: 1463-1465 (1998).

[51] T.S.K.So and C.W.Huie. Investigation of the effects of cyclodextrin and organic solvents on the separation of cationic surfactants in Capillary Electrophoresis. *J. Chromatography A.* **872**: 269-278 (2000).

[52] G. Kavran and F.B. Erim. Separation of polycyclic aromatic hydrocarbons with sodium dodecylbenzensulfonate in electrokinetic chromatography. *J. Chromatography A.* **949**: 301-305 (2002).

[53] L. Křivánková, P. Gebauer and P. Boček. Some practical aspects of utilizing the on-line combination of isotachophoresis and capillary zone electrophoresis. *J. Chromatography A.* **716**: 35-48 (1995).

[54] .R.J. Vecchio. Understanding Design of Experiments. Carl Hanser Verlag, Munich. 1997, pp. 1-173.

[55] D.M. Byrne and S. Taguchi. The Taguchi Approach to Parameter Design. American Society for Quality Control, Inc. Milwaukee, Wisconsin. (1987).

[56] N.Logothetis and A. Haigh. Characterizing and Optimizating multi-response processes by the Taguchi Method. Quality and Reliability Engineering International. **4**: 159-169 (1988).

[57] F. Box, S. Bisgaard and C. Fung. An Explaination and Critique of Taguchi;s contributions to Quality Engineering. Quality and Reliability Engineering International. **4**: 123-131 (1988).

[58] A. C. Shoemaker and R. N. Kacher. A Methodology for Planning Experiments in Robust Product and Process Design. Quality and Reliability Engineering International. **4**: 95-103 (1988).

[59] W.P Gardiner and G.Gettinby. Experimental Design Techniques in Statistical Practise, A Practical Software-based Approach. Horwood Publishing. 1998, pp 289-321.

[60] G.Taguchi, D. Clausing. System of Epxerimental Design Engineering Methods to Optimize Quality and Minimize Costs. Vol 1. UNIPUB, Kraus International Publications, 1988, pp. 117-236.

[61] G.Taguchi, D. Clausing. System of Epxerimental Design Engineering Methods to Optimize Quality and Minimize Costs. Vol 2. UNIPUB, Kraus International Publications, 1988, pp. 585-730.

[62] G.R. Bandurek and J. Disney and A. Bendell. Application of Taguchi Methods to Surface Mount Processes. Quality and Reliability Engineering International. **4**: 171-181 (1988).

[63] ANOVA-TM for Windows and ANOVA-TM Professional, Advanced Systems and Designs, Inc. USA, 1984-96.

[64] 'SEMI' suggested Guidelines for Pure Water for Semiconductor processing, in SEMI Suggested Guidelines, 1995, pp.201.

[65] K.Heinig and C. Vogt. Determination of surfactants by capillary electrophoresis. *Electrophoresis.* **20**: 3311-3328 (1999).

[66] J.Riu, P. Eichhorn, J.A. Guerrero, Th. P. Knepper and D. Barceló. Determination of Linear alkylbenzenesulfonoates in wastewater treatment plants and coastal waters by automated solid-phase extraction followed by capillary electrophoresis-UV detection and confirmation by capillary electrophoresis-mass spectroscopy. *J. Chromatography A.* **889**: 221-229 (2000).

[67] K. Heinig, C.Vogt. and G. Werner. Trace analysis of surfactants using chromatogratographic and electrophoretic techniques. *Freseiu J. Anal. Chem.* **361**: 612-618 (1999).

[68] V.Verhelst, J.-P. Mollie, F. Campeol. Capillay zone electrophorestic of ionic impurities in silicon products used for electronic applications. *J. Chromatography A.* **770**: 337-344 (1997).